Deltares

DC project Bijzondere Belastingen

Soil response during an explosion in a tunnel

Piet Meijers

© Deltares, 2009

Deltares

Title
DC project Bijzondere Belastingen

Client	Project	Reference	Pages
Consortium Delft COB	Cluster1001136-006	1001136-006-GEO-0001	**Error! Reference source not found.**

Keywords
Tunnel, explosion, Biot, soil response

Summary
The dynamic response of soil around a tunnel is investigated using the newly developed Biot implementation in PLAXIS. The tunnel is loaded internally by a BLEVE. The resulting shear strains indicate that is loose sand residual excess pore pressures may be present after the blast. The consequences for the surrounding are not investigated.

References

Version	Date	Author	Initials	Review	Initials	Approval	Initials
	12-10-2009	Piet Meijers		Paul Hölscher		Marco Hutteman	

State
draft
This report is a draft report, not a final report and for discussion purposes only. No part of this report may be relied upon by either principal or third parties.

CONSORTIUM DC-COB

Contents

1 Introduction

1.1 Background of the project

In the Netherlands the available land is used more and more intensively. Main corridors of transport (roads and railroads) are part of the urban area. In order to avoid the negative influences of the corridors of transport (noise, pollution, barriers for local transport) many main corridors of transport will be built in tunnels.
The responsible authorities have to decide whether dangerous goods may be transported through these tunnels. Firstly, their attention focuses on the safety of human beings in the tunnel. However, also the integrity of the structure and the economic consequences of an accident must be considered. For the last aspect, good knowledge of the loading mechanism and the structural response is required.

Nowadays the goods which are sensitive for explosion are transported along alternative routes that exclude tunnels. These are mostly secondary roads. The transport along these alternative roads has many disadvantages, such as the safety along the route, the air- and noise pollution along the road and the higher transport costs. Therefore, it is preferred to permit the transport of dangerous goods through tunnels. In case of multiple use of space this leads to the question what are the possible consequences and risks for buildings and other structures above the tunnel.

In this Delft Cluster work package “Bijzondere Belastingen” (CT01.21) the consequences of an accident with the transport of explosion hazardous goods are considered: BLEVE (Boiling Liquid Expanding Vapour Explosion) and gas explosion. These phenomena have a low probability of occurrence, but might have immense consequences. Therefore, a deterministic consideration is not possible.

The results of the work package must facilitate the quantitative risk analysis of the phenomena, which supports the authorities in their decision of allowing transport of dangerous goods through tunnels or not. The work package focus is on the mechanical description of the loading and the response. However, it requires an interdisciplinary approach, which integrates knowledge of risk analysis, explosion and evaporation of liquid gases, structural dynamics and dynamics of soil.

1.2 Project description

The work package plan contains two main stream research lines:

1. Loading due to BLEVE and gas explosion. The BLEVE research is mainly executed in a PhD-study at Delft University of Technology. This part focuses on an improved understanding and modelling of the BLEVE phenomenon. TNO Defence and Safety will participate in this research line by introduction of practical mechanical modelling of the vessel behaviour and creation of a practical engineering model for a BLEVE load, based on the results of the PhD-study.
2. Dynamical Response of the structure-soil system under loading by a BLEVE and gas explosion loading. Here TNO Built Environment and Geosciences concentrates on the structural part of the problem, while Deltares and Delft University of Technology will take care of the soil response. TNO Defence and Safety will provide data on appropriate loads for realistic cases.

The project is divided into the following sub work packages:

- L1: Mechanical aspects of the initiation of a BLEVE
- L2: Thermodynamic and gas dynamic aspects of a BLEVE
- R1: Preliminary structural response
- R2: Soil behaviour
- R3: Full system response
- R4: Consequences for surroundings (cancelled)

This report is part of sub work package R3.

1.3 Aim of work package R3

Sub work package R3 aims at integrating the tunnel response and the soil response due to blast loading.

1.4 Scope of this report

During a BLEVE both the tunnel and the surrounding soil are dynamically loaded by a heavy load. Both the tunnel and the soil should be modelled in a sophisticated way. At this moment The simulation of the response of the fully coupled tunnel-soil system cannot be solved within one advanced program. Simplifications in the modeling of the soil or the tunnel are always required. The required simplifications are model dependant. In work package R3 the consequences of these simplifications are studied.

Therefore, two calculation models are compared:

- a model with an advanced description of the tunnel and a basic model of the soil. This work is done by TNO using the FEM program LS-DYNA
- a model with an advanced description of the soil and a basic model of the tunnel. This work is done by Deltares using the FEM program Plaxis, this report describes the results of the work done by Deltares.

In this report the soil is modeled using the Biot description of soil. In this model, the fluid and skeleton in the sand are distinct materials, with interaction. Therefore, the decisions whether the material behaves drained or undrained don't need to be made before hand. The 'amount' of drainage is a result of the calculation. For this simulation the FEM model Plaxis was used. Plaxis allows modeling the tunnel with basic constitutive models only.

2 Starting points

2.1 General

The calculations for the soil response are made with the program PLAXIS and the BIOT implementation, as developed as part of this DC project.

2.2 Geometry tunnel

For the geometry of the tunnel the Thomassen tunnel (formerly known as Caland tunnel) is used. Figure 2.1 shows the dimensions of the tunnel.

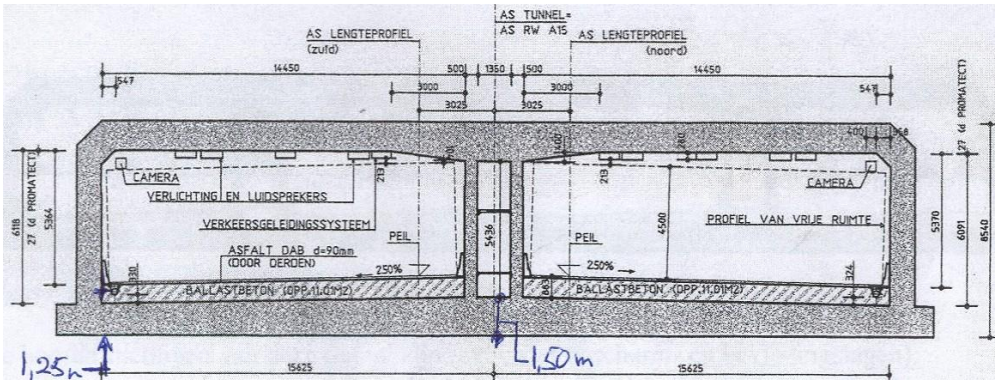

Figure 2.1 Dimensions cross section Thomassen Tunnel

A sand cover of 2 m is assumed. In the PLAXIS calculations the ground water table is taken equal to the ground level.

For the calculations the shape is somewhat simplified. The actual used geometry is shown in section 4.4.

2.3 Loading

For the blast loading ae BLEVE loading and a gas explosion are used. The numerical data are given in table 2.1. A graph of the load as function of time is shown in figure 2.2 and 2.3.

BLEVE load		gas explosion	
Time [s]	Pressure [kPa]	Time [s]	Pressure [kPa]
0	0	0	0
0.00001	513	0.00001	1617
0.02	130	0.0328	410
0.08	30	0.1312	95
0.15	0	0.246	0
1	0		

Table 2.1 Blast loading

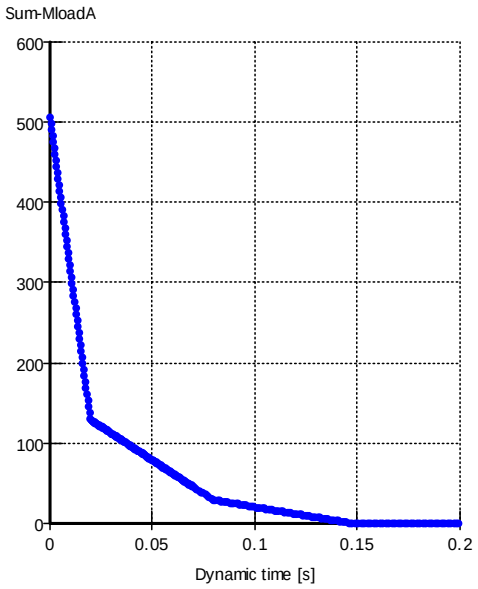

Figure 2.2 Blast loading, BLEVE

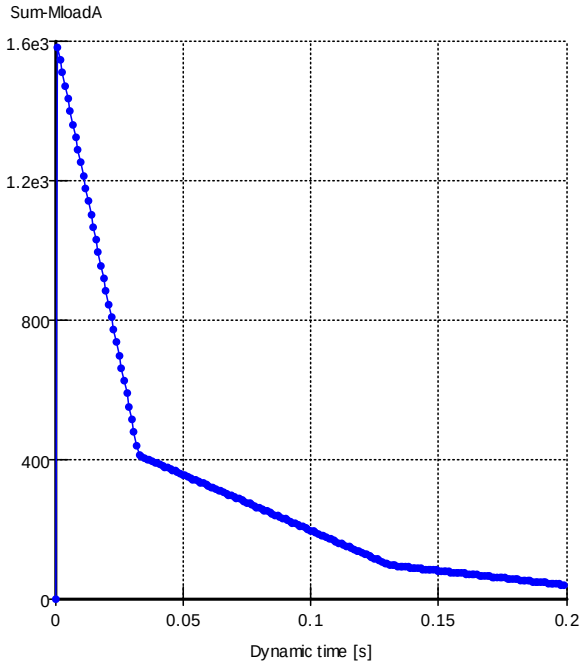

Figure 2.3 Blast loading, gas explosion

2.4 Soil parameters

In the calculations a homogeneous subsoil, consisting of sand, is assumed. For the constitutive model of the sand the so called hardening Soil model is used. This soil model is selected as it uses a stress dependent stiffness and different loading and unloading-reloading stiffness. A full description of the Hardening Soil model is given in the PLAXIS material model manual [PLAXIS

The relevant soil parameters are derived from performed triaxial tests with fast loading-unloading. The derivation of the soil parameters is described in chapter 3.

3 Selection soil parameters

3.1 Results triaxial testing

The results of the triaxial tests are described in Deltares report 418420.0026 [Meijers 2007]. The results of these tests are used to select the soil parameters for the FEM calculations. In this chapter the selection of these paramameters is described.

The density of the sand in the tests was medium dense (test 1 to 3) and loose (test 4 to 5B). Slow and fast loading unloading was used in the triaxial tests.
It appeared from the tests that, within the used deformation velocities, the loading rate had no significant influence on the average soil response.
During unloading the pore pressure was found to increases.

3.2 Fitting triaxial test results with PLAXIS

The dimensions of the test sample in the triaxiaal tests are:

- height: 0.15 m
- diameter: 0.066 m

On top of the sand a stiff plate (top platen) is modelled.

The sample is modelled using an axial symmetric mesh with 6-node triangular elements. Figure 3.1 shows the mesh.

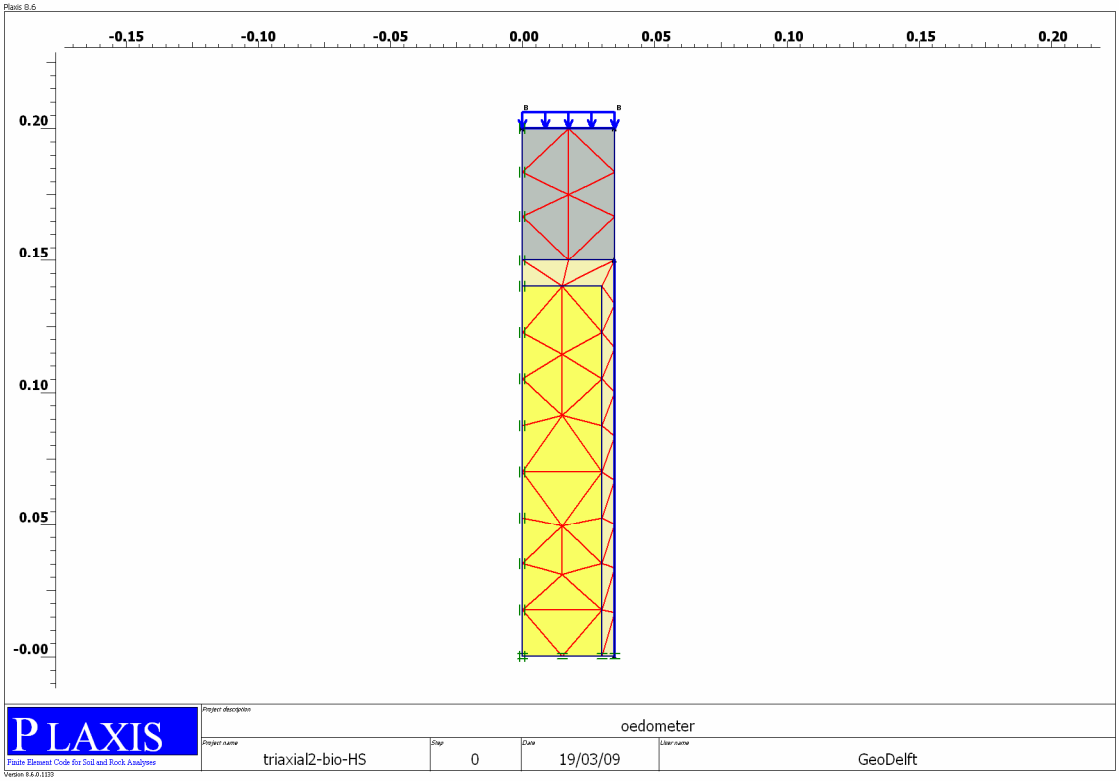

Figure 3.1 Used mesh for modelling triaxial tests

The following boundary conditions are applied:

- symmetry axis: free vertical movement, no horizontal movement
- bottom: free horizontal movement, no vertical movement
- top of sand sample: fixed at top platen
- right boundary: free horizontal and vertical movement, prescribed boundary stress

The initial stress (consolidation stress) is modelled by prescribing a horizontal stress at the side and a vertical load at the top of the mesh.

The dynamic loading is modelled as a prescribed stress at the top of the mesh. For this the measured time-stress in the tests is used. A stress controlled calculation is used as with a displacement controlled calculation the moment of unloading (disconnecting of the plunger from the top platen) is hard to define.

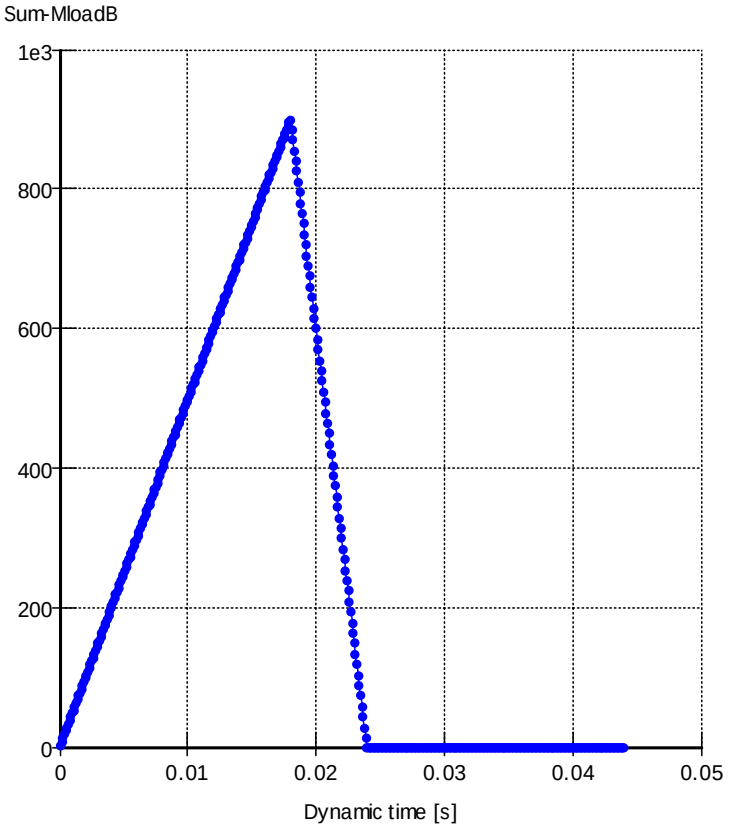

Figure 3.2 Applied time stress curve

3.3 Fitting test 1, medium dense sand

The stress amplitude is taken from the measured stress amplitude during the test. A value of 900 kPa is used for the tests on medium dense sand.

Figure 3.3 shows the measured vertical stress-vertical strain loop in test 1 (medium dense sand, slow loading).

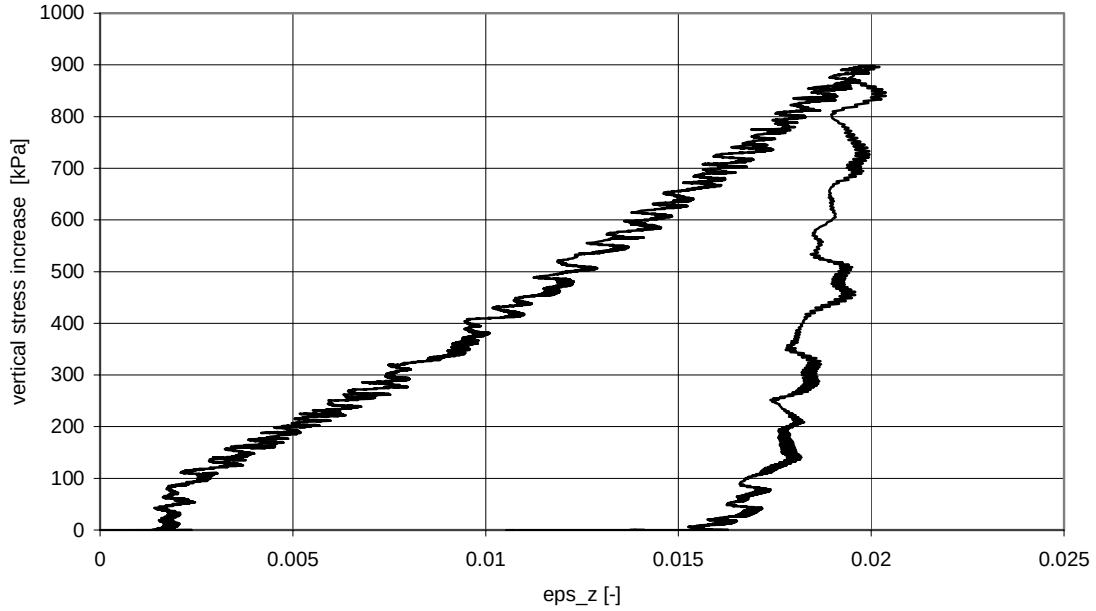

Figure 3.3 Measured vertical stress-strain behaviour test 1 (medium dense sand)

The strength parameters cannot be derived from the test results. Use is made of correlations with the relative density. For the medium dense sand (Re = 0.7) this gives:

- $\phi = 37.5°$
- $\psi = \phi - 30° = 7.5°$

A first estimate of the stiffness parameters is made using the measured stress-strain response in the tests. As these parameters did not yield the correct stress-strain behaviour in the calculations a trial-and-error is followed. From this approach the following values are selected:

- $p_{ref} = 100$ kPa
- $m = 0.5$
- $E_{50}^{ref} = 130$ MPa
- $E_{oed}^{ref} = 152$ MPa (limit by PLAXIS)..
- $E_{ur}^{ref} = 260$ MPa (lowest permissible value with given E_{50}^{ref})

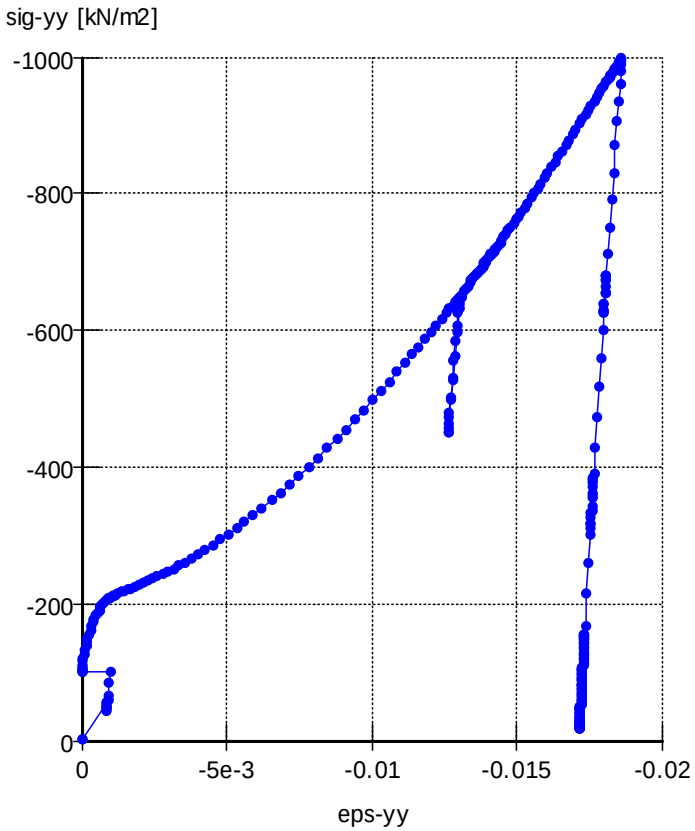

Figure 3.4 Stress-strain behaviour in simulation loading-unloading medium dense sand

The resulting stress-strain plot is shown in figure 3.3. The strain at loading is correct. This is not surprising as the stiffness parameters are selected thus that this strain is obtained. The unloading stiffness is higher as obtained from the test results.
The apparent unloading step at a vertical stress of about 600 kPa is remarkable. Inspecting the time-displacement curve of the top platen shows a slight upward movement of the top platen at the same time. A calculation with a slower loading doesnot show this type of behaviour. It is expected that this behaviour is due to the dynamic behaviour of the system.

For further comparison of the measured and calculated soil response the effective stress path and the development of the pore pressure are shown in the figures 3.4 to 3.7.

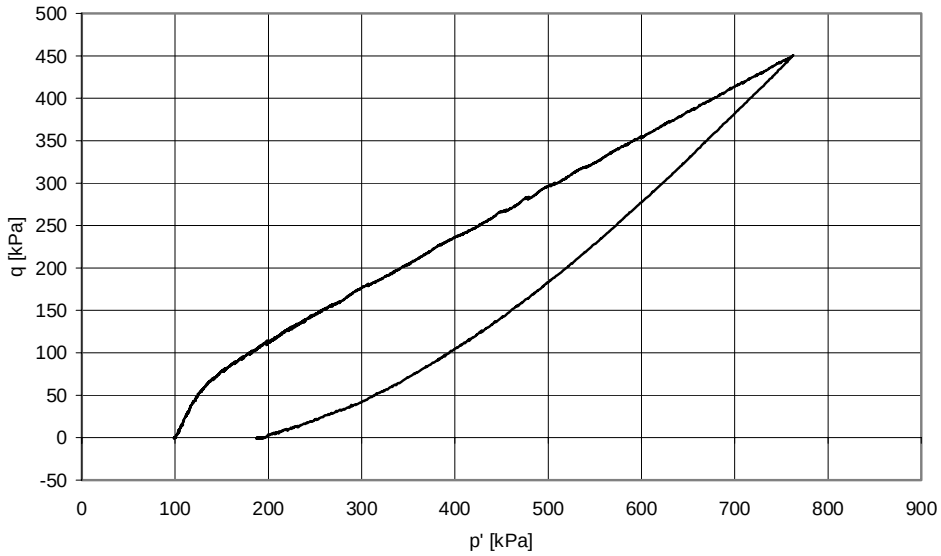

Figure 3.5 *p' – q plot test 1*

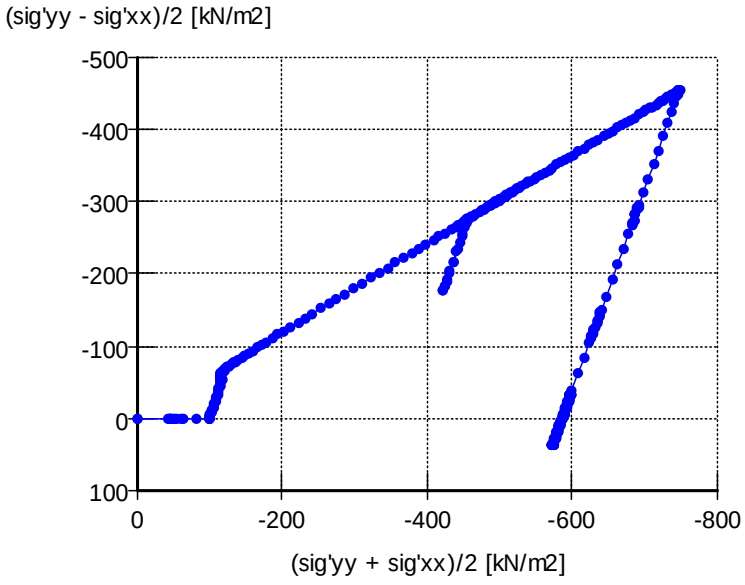

Figure 3.6 *p'-q plot calculation*

The loading part in the stress path plot resembles the measured path. The unloading part yields a much higher residual p' as observed in the test. This indicates that the pore pressure in the calculation is less than in the test.

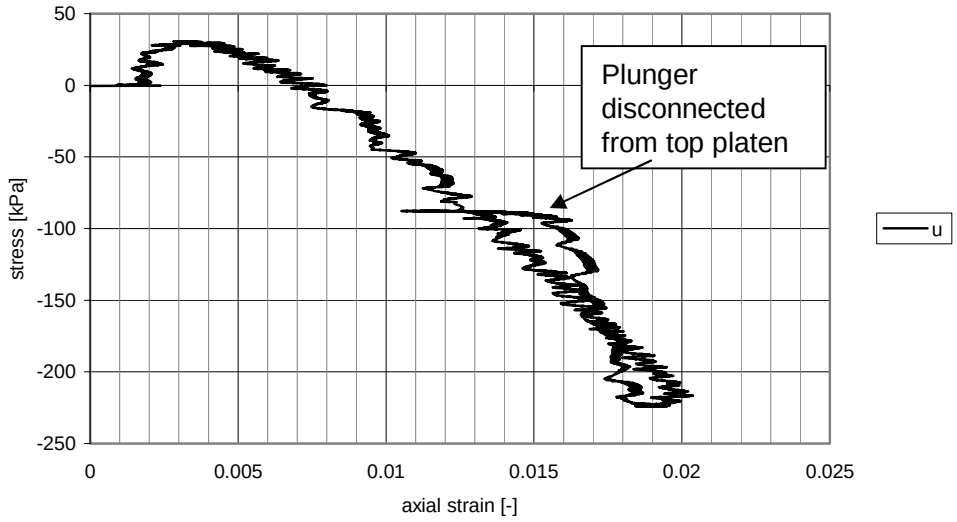

Figure 3.7 *Development excess pore pressure in test 1*

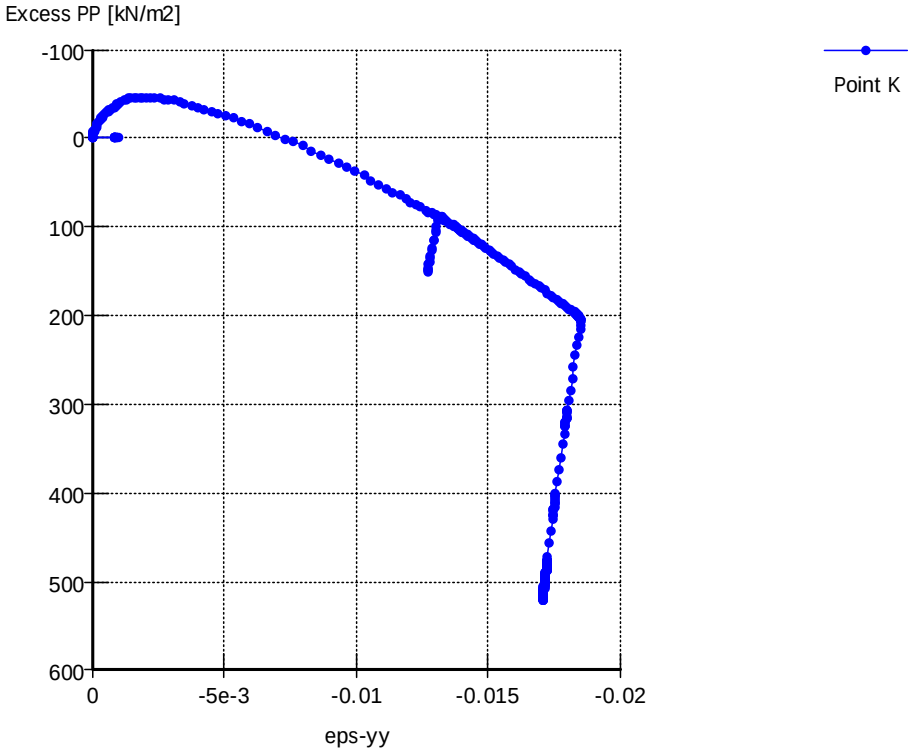

Figure 3.8 *Development excess pore pressure in the calculation*

The development of the excess pore pressure during loading resembles the measured value. At unloading the behaviour is quite different. In the test the excess pore pressure increases (becomes less negative). In the calculation the excess pore pressure becomes more negative at unloading (please note the different sign convention in the test results and in the PLAXIS calculations).

3.4 Fitting test 4, loose sand

Also for the test with loose sand the stiffness parameters needed to obtain in the PLAXIS simulation the same stress-strain behaviour as in the test are derived.

Selected strength and stiffness parameters for test 4 are:

- $\phi = 32.5°$
- $\psi = 2.5°$
- $E_{50}^{ref} = 90$ MPa
- $E_{oed}^{ref} = 90$ MPa
- $E_{ur}^{ref} = 180$ MPa
- $p_{ref} = 100$ kPa (stress for which the reference stiffness is valid)
- m = 0.5 (power in stress stiffness relation)

Note:

- the applied maximum additional stress is 200 kPa, the maximum vertical stress thus becomes 300 kPa
- when using the measured time-stress curve from the tests a maximum stress of 350 kPa is reached in the simulation at t = 0.02 s, this implies an overshoot of the stresses; therefore the load curve is adjusted by multiplying the time scale with a factor of 10
- the achieved maximum strain is not only influenced by the stiffness parameters but also by the strength parameters, most likely because dilatancy is generated; decreasing the strength parameters increases the strain
- the selected soil stiffness is much larger as would be estimated from correlation with the relative density
- in the test results the stiffness of the first part (before yielding) is much higher as the selected soil stiffness

The next figures show the result in the test and the result in the PLAXIS simulation.

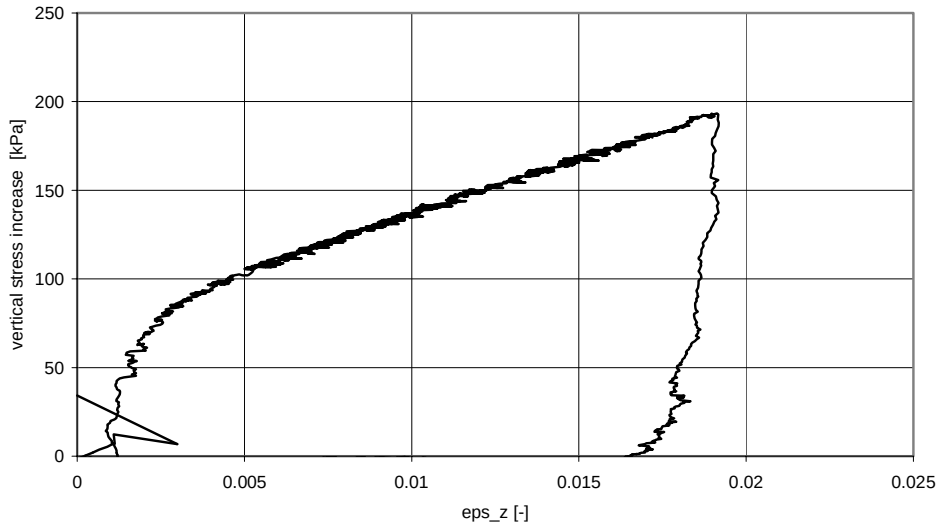

Figure 3.9 Vertical stress strain behaviour test 4 (loose sand)

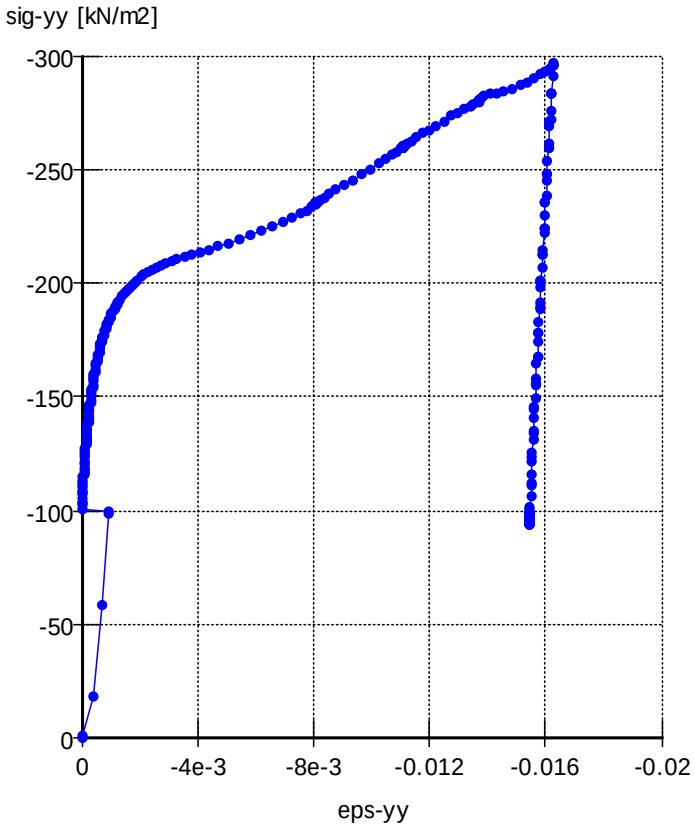

Figure 3.10 *Vertical stress-strain development in the calculation*

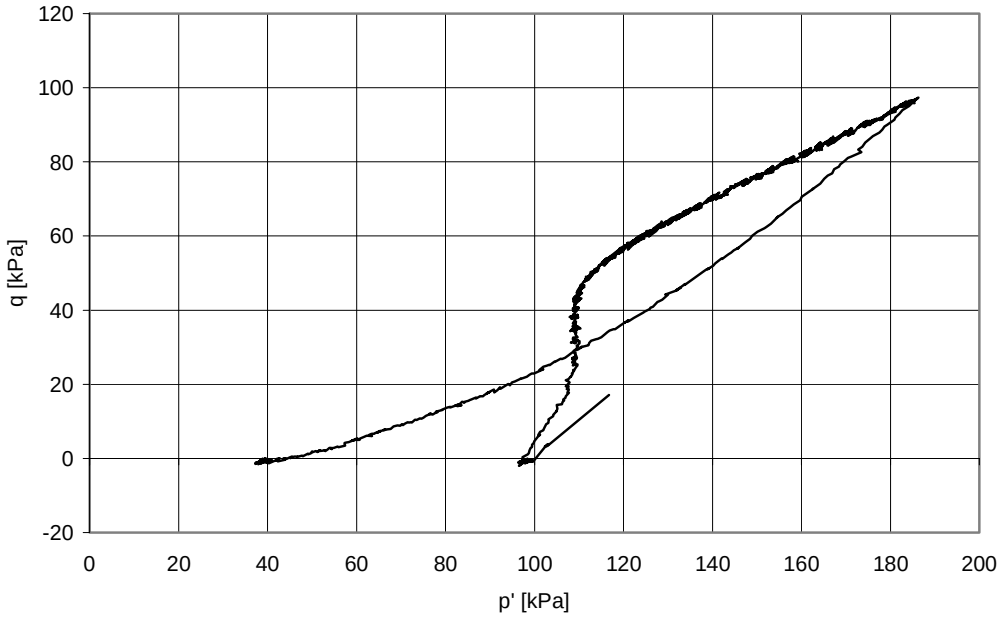

Figure 3.11 *p' – q plot test 4*

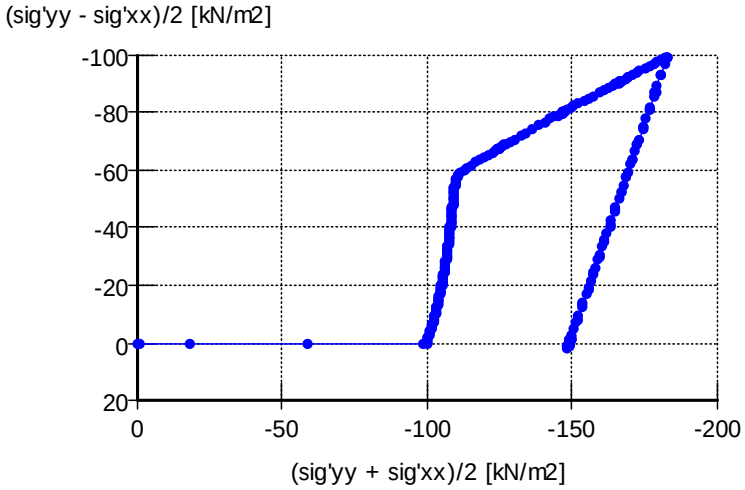

Figure 3.12 *p'- q plot in the calculation*

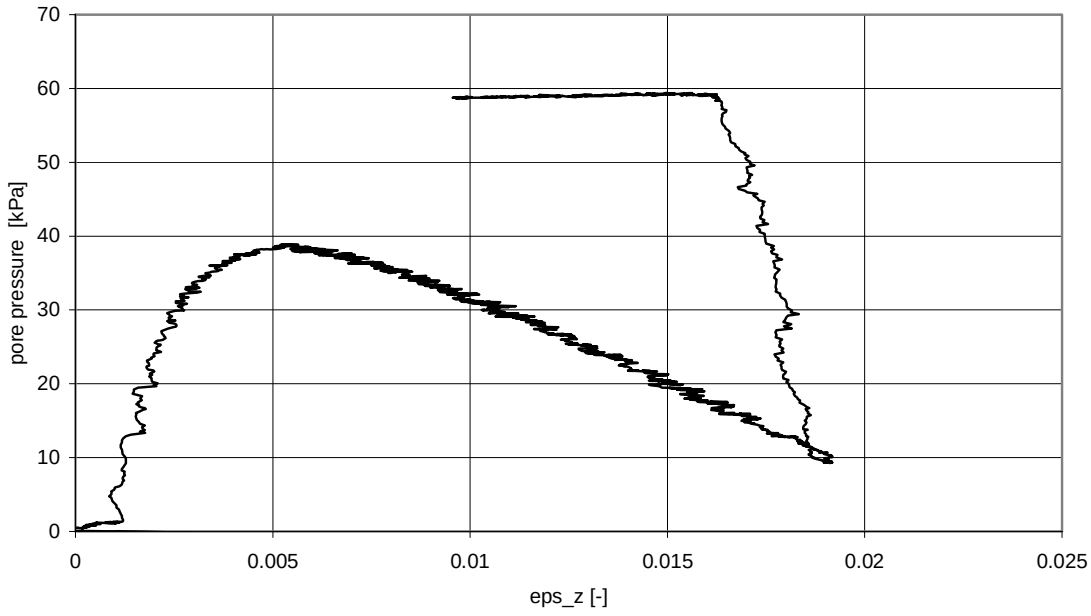

Figure 3.13 *Development excess pore pressure test 4*

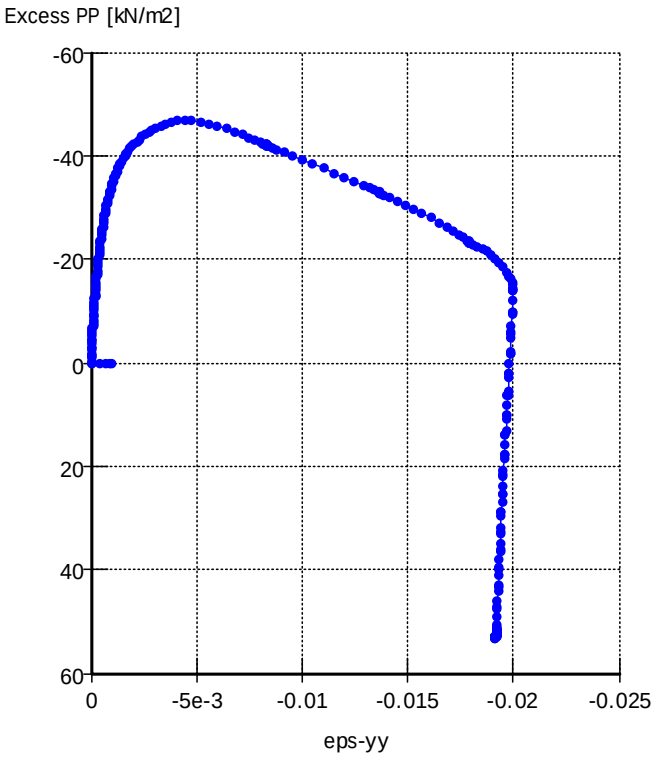

Figure 3.14 Development excess pore pressure in the calculation

The calculated soil response at loading corresponds reasonably with the measured response. The maximum pore pressure in the calculation is a little above the measured pore pressure.

As with the other test, the calculated development of the excess pore pressure at unloading differs from the measured development. In the calculation the pore pressure decreases while in the test it increases. This is a shortcoming of the used (and available) constitutive models in PLAXIS. The consequence will be that at large loading followed by unloading the pore pressures are underestimated.
This difference in the development of the pore pressure is believed to be responsible for the difference in the stress path at unloading.

3.5 Conclusions

The calculated soil response at loading corresponds reasonably with the measured response.

For the unloading stage the calculation results show a decrease in the water pressure decreases. This is consistent with the assumption in the used soil model that at unloading the soil behaves linear-elastic. An undrained unloading results in such a model in a decrease in the pore pressure.
In the triaxial tests an increase in the pore pressure is observed during unloading. From this follows that the model doesnot properly predict the soil behaviour at unloading. The consequences will be described in chapter 7.

4 Outline calculations soil-tunnel response with PLAXIS

4.1 Calculation procedure

In the PLAXIS calculation the tunnel and soil are modelled with 6-node triangular elements. No interface element is used between tunnel and soil.

The following phases are used:

1 initial phase, no tunnel
2 excavation of trench for submerged tunnel
3 installation of tunnel
4 backfilling of trench
5 explosion loading

For phase 1 to 4 the soil is assumed to behave drained. For phase 5 the soil is assumed to behave undrained. In the calculation the history of the tunnel is followed, as this may influence the soil behaviour when using an elasto-plastic soil model.

4.2 Soil parameters

The used soil model is the Hardening Soil model. The following soil parameters are used:

- E_{50}^{ref} = 130 MPa
- E_{oed}^{ref} = 152 MPa
- E_{ur}^{ref} = 260 MPa
- P_{ref} = 100 kPa
- m= 0.5
- ν_{ur} = 0.2
- ϕ = 37.5°
- ψ = 7.5°
- γ_{wet} = 20 kN/m^3

In PLAXIS a Rayleigh damping is used for the material damping. For the sand the following parameters are used:

α = 0.12
β = 0.0001

The resulting frequency dependent material damping is shown in figure 4.1.

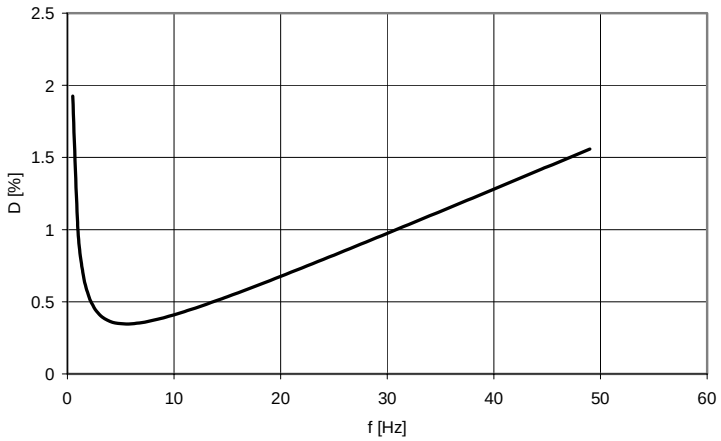

Figure 4.1 Material damping sand as function of frequency

4.3 Tunnel parameters

The tunnel is modelled with volume elements. The material is modelled as 'non-porous'.

The available soil models in PLAXIS do not allow to model the elasto-plastic behaviour of concrete correctly. Most calculations are made using a linear-elastic non-porous material model with the following parameters:

- E = 10 GPa (cracked concrete, recommended value by TNO)
- $\nu = 0.15$
- $\gamma = 25$ kN/m^3

The material damping of the concrete is set to zero.

For one situation the effect of plastic concrete behaviour is checked. A Mohr-Coulomb material model is used with the following additional parameters:

- c = 10 MPa
- tensile strength: 6 MPa
- $\phi = 0°$
- $\psi = 0°$

4.4 Mesh and boundary conditions

Figure 4.2 and 4.3 show the used mesh. The following boundary conditions are used:

- lower boundary: horizontal and vertical displacements are zero
- outer boundary: horizontal displacements are zero, vertical displacements are free
- top boundary: displacements are free, pore pressure is 0 kPa

No absorbing boundaries are used as the combination of Biot with viscous boundaries is not allowed. For this reason a large width and height of the mesh are selected, in order to limit boundary effects.
The groundwater table is taken equal with the top of the mesh.

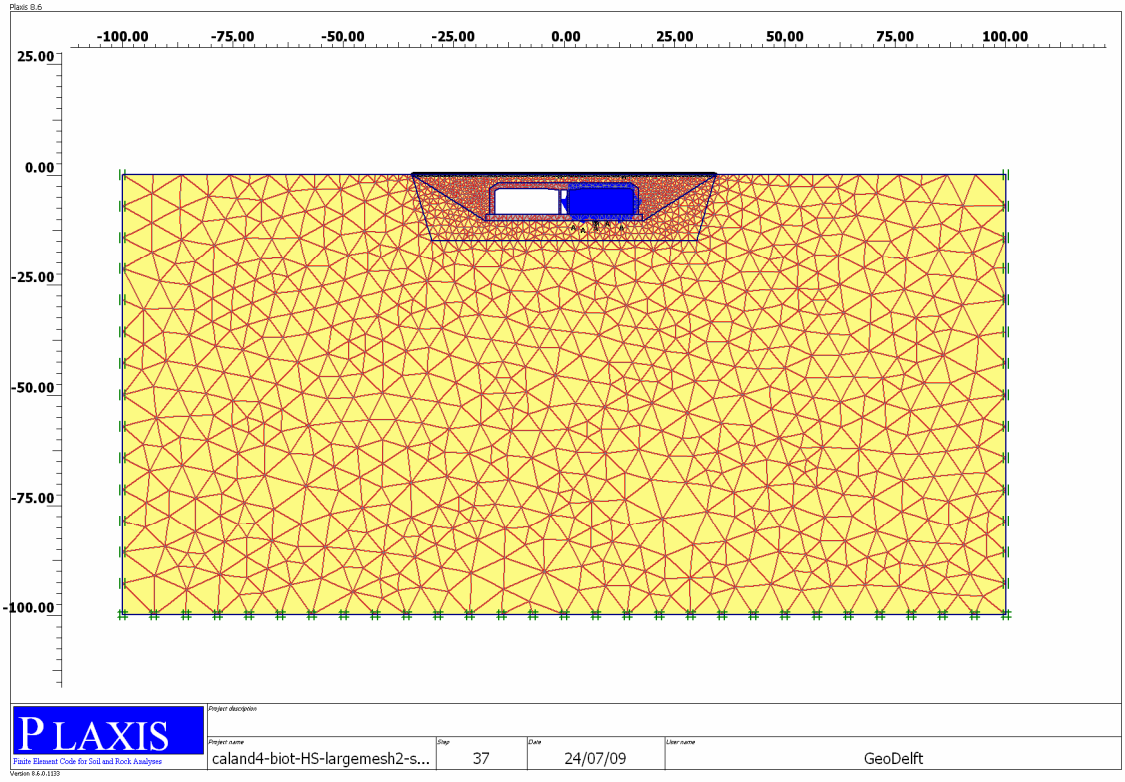

Figure 4.2 *Mesh for the tunnel calculations*

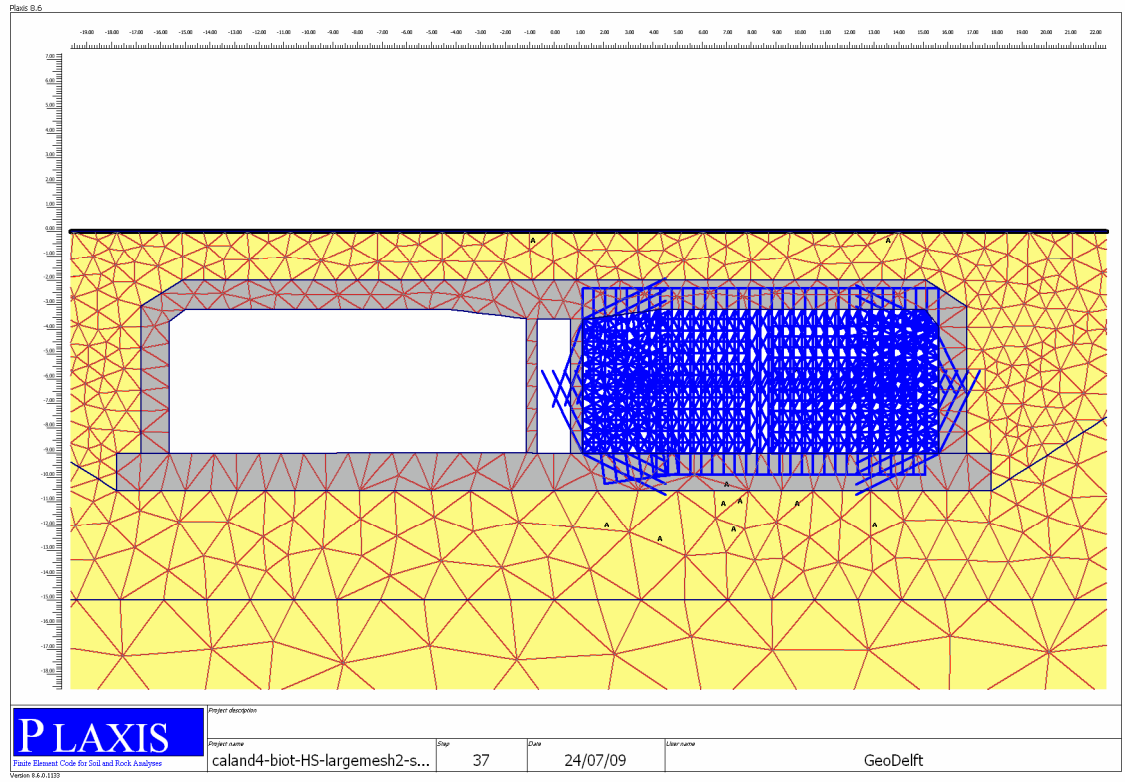

Figure 4.3 *Mesh for the tunnel calculations (detail)*

5 Calculation results

5.1 General

This chapter presents the calculated tunnel and soil response with PLAXIS. The following situations are considered:

1 response of a LE tunnel without soil
2 response of an LE tunnel in soil, blast load 500 kPa,without BIOT
3 response of an LE tunnel in soil, blast load 500 kPa,BIOT option used
4 response of an LE tunnel in soil, blast load 1600 kPa, BIOT option used
5 response of an LE-plastic tunnel in soil, blast load 500 kPa, BIOT option used
6 response of an LE-plastic tunnel in soil, blast load 500 kPa, BIOT option used, reduced soil strength and stiffness

Calculation 1 serves to show the tunnel response in PLAXIS and compare the response with previous calculations by TNO [Vervuurt et al 2007]. Results are described and discussed in section 5.2.

Calculation 2 and 3 serve to show the effect of soil on the tunnel response and to show the effect of using the BIOT option on the tunnel and soil response. Results are described and discussed in section 5.3.

Calculation 4 serves to show the effect of a larger blast load on the tunnel and soil response. Results are described and discussed in section 5.4.

Calculation 5 serves to show the effect of elasto-plastic tunnel behaviour on the tunnel response in PLAXIS. This calculation is to be compared with the TNO calculations with LS-DYNA (reference TNO report 2009 to be added). Results are described and discussed in section 5.5.

Calculation 6 serves to show the effect of soil parameters on the tunnel and soil response. Results are described and discussed in section 5.6.

run	name	soil behaviour	tunnel behaviour	max. explosion pressure [kPa]
1a	caland-tunnelonly.plx	no soil	LE	500
1b	caland-tunnelonly-largeelements.plx	no soil	LE	500
2a	caland5-run2a.plx	drained soil	LE	500
2b	caland5-run2b.plx	undrained soil	LE	500
3	caland5-run3.plx	Biot	LE	500
4	caland5-run4.plx	Biot	LE	1600
5	caland5-run5.plx	Biot	elasto-plastic	500
6	caland5-run6.plx	Biot, reduced soil strength and stiffness	elasto-plastic	500

Table 5.1 Overview calculations

5.2 Comparison tunnel response PLAXIS and DIANA

Calculation 1 serves to show the tunnel response in PLAXIS and compare the response with previous calculations by TNO.

In the calculations by [Vervuurt et al 2007] with DIANA the tunnel is modelled with beam elements. In the present calculations the tunnel is modelled with volume elements. In order to check the effect of this different modelling on the tunnel response one calculation is made with a non-embedded tunnel with linear-elastic material behaviour.

The response according to the DIANA simulation is shown in figure 5.1.

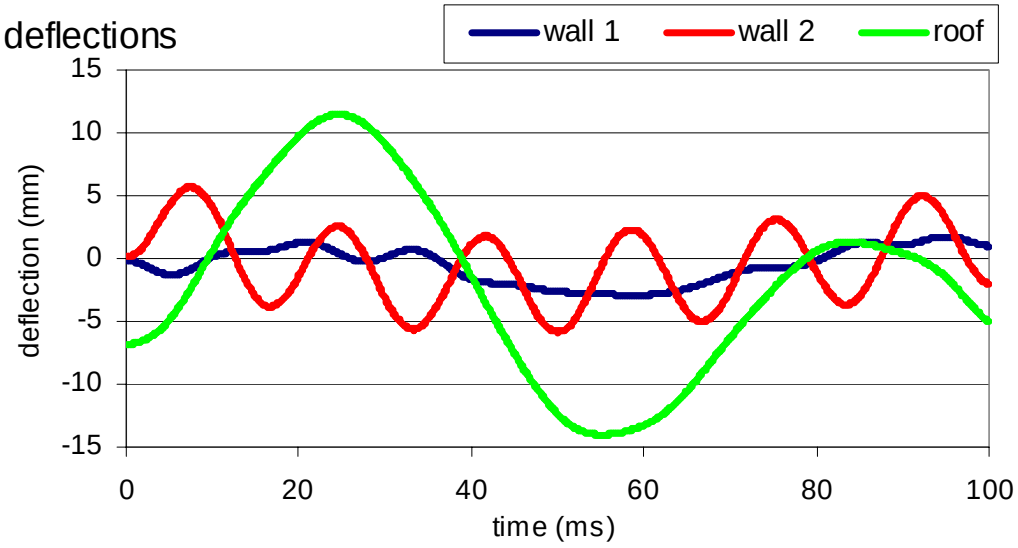

Figure 5.1 Tunnel response, DIANA calculation (figure 21 of 2007-D-R0156)

Dimensions and loading of the tunnel are chosen identical to the DIANA simulation.
The following parameters are used in the PLAXIS simulation:

- E = 31 GPa
- ν = 0.15
- ρ = 2500 kg/m^3

As in the TNO calculations the tunnel roof is fixed (not deformable) the floor of the tunnel is fixed, both horizontal and vertical. Figure 5.2 shows the PLAXIS mesh.

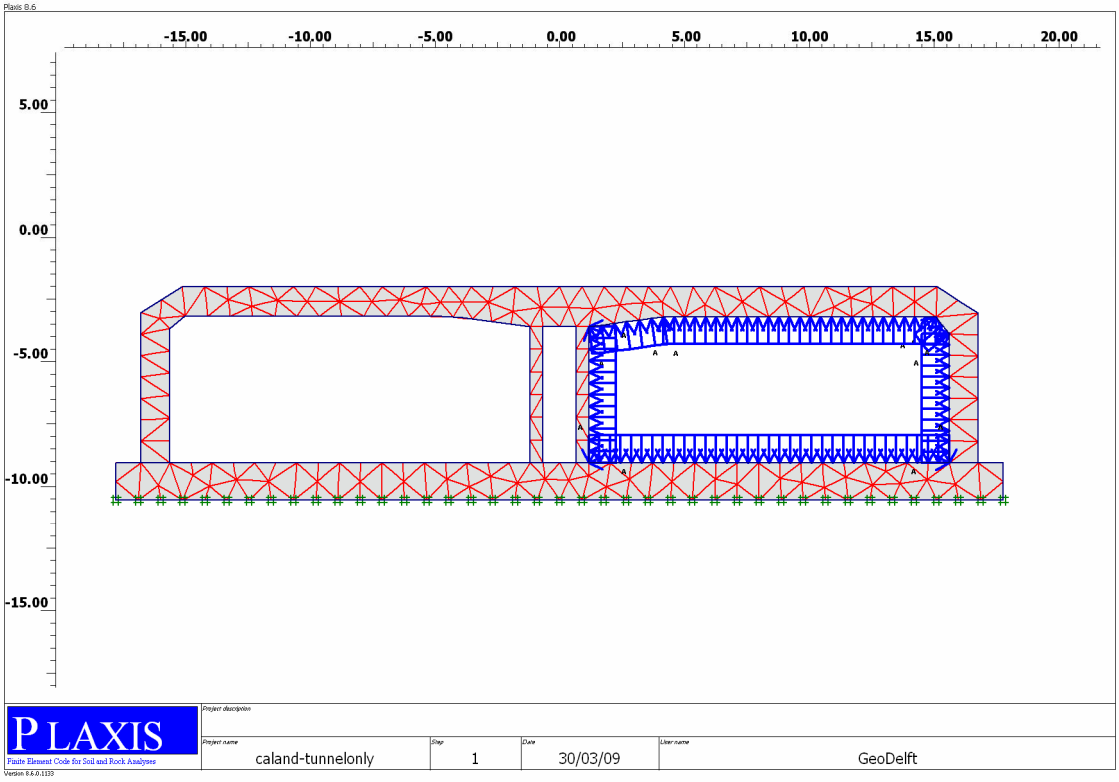

Figure 5.2 *PLAXIS mesh for assessment tunnel only*

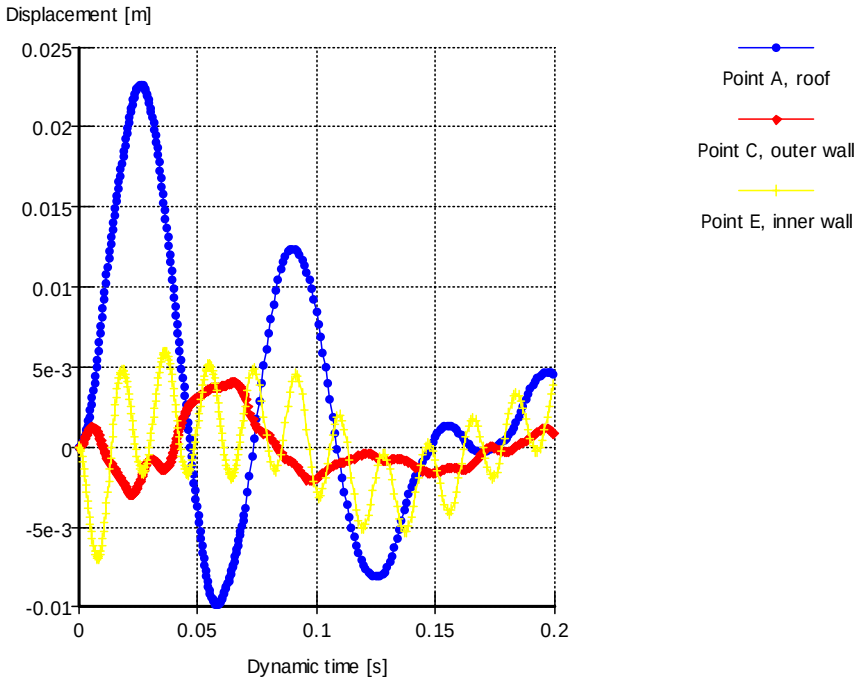

Figure 5.3 *Tunnel response, E = 31 GPa*

The tunnel response according to PLAXIS with volume elements is in fair agreement with the tunnel response according to DIANA with beam elements.

Please note that the outer wall at first moves in the positive direction (outward), in the direction of the applied stress. Very soon however it starts to move inwards, in the direction opposite to the applied stress. Reason for this behaviour is the upward movement of the roof, resulting in a rotation at the corner roof-outer wall. This in turn results in an inward movement of the outer wall.
At the inner wall the displacement is in the negative (outward) direction. The thinner inner wall is more flexible as the outer wall. This prevents a movement of the wall in the direction opposite to the applied stress.

The calculations in the next sections will be made using E = 10 GPa, as recommended by TNO. For comparison also a the response of the tunnel with this lower stiffness is determined. Figure 5.4 shows the results.

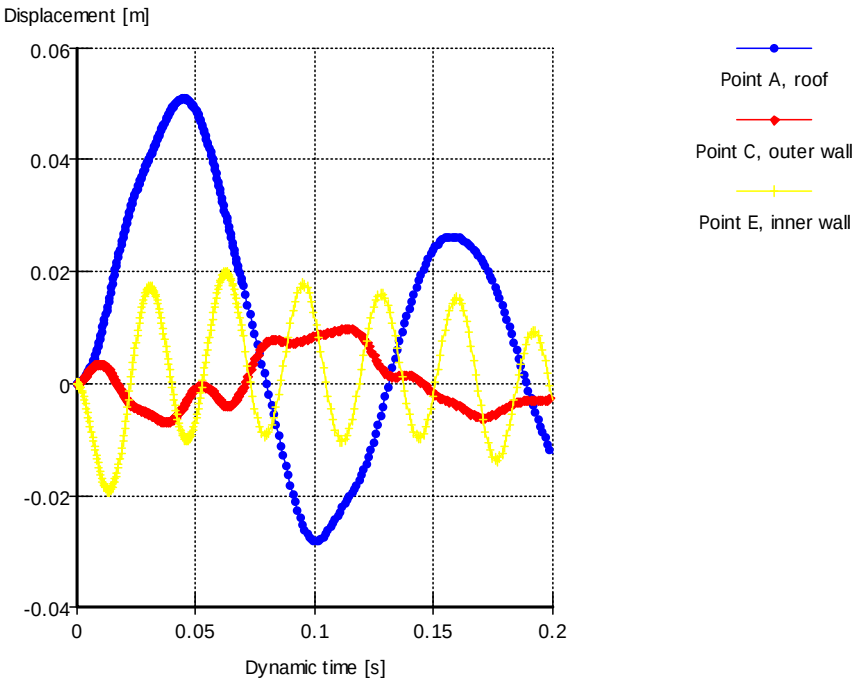

Figure 5.4 Tunnel response, E = 10 GPa

The frequency of the response decreases and the amplitude increases with decreasing stiffness of the concrete.

In order to check the element size on the tunnel response a calculation with relatively large elements is made as well. The mesh is shown in figure 5.7 and the tunnel response in figure 5.8.

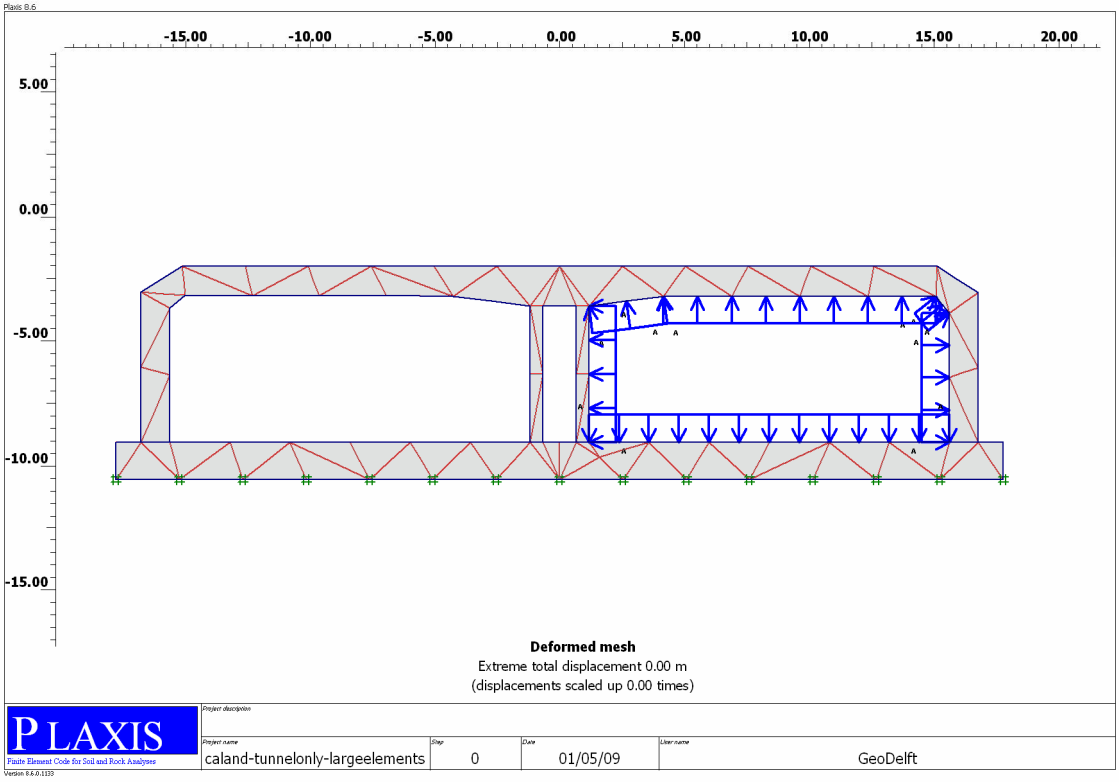

Figure 5.5 Tunnel mesh with large elements

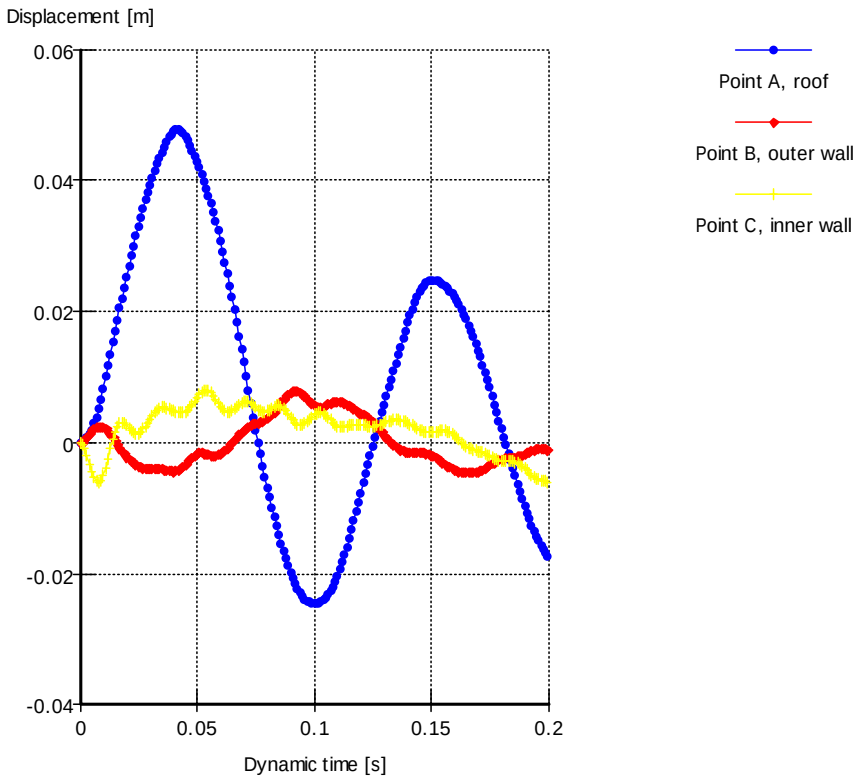

Figure 5.6 Tunnel response when using large elements

Comparing figure 5.6 with 5. 4 shows that the response of the roof and outer wall are in fair agreement. The response of the inner wall differs greatly differs, probably due to the extreme length-height ration of the elements of the inner wall.

5.3 Effect soil on tunnel response

Calculation 2 and 3 serve to show the effect of soil on the tunnel response and to show the effect of using the BIOT option on the tunnel and soil response.

In this section three calculations are discussed. The variation in the calculatiosn is the used soil model. The respons of the tunnel for the following variations are investigated:

- - undrained soil behaviour, no use of BIOT option
- - drained soil behaviour, no use of BIOT option
- - soil behaviour using BIOT option

The difference between the drained and the undrained soil behaviour is that in the first option the water pressure is always equal to the hydrostatic stress and the load is taken by the soil skeleton only. In the second option the load is taken by the water and the soil skeleton.

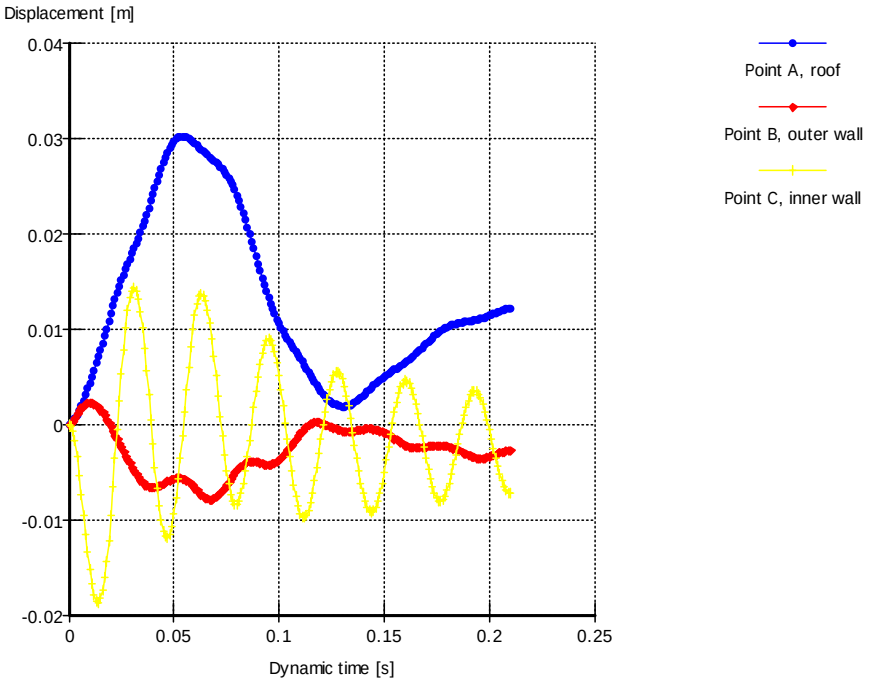

Figure 5.7 Tunnel response, blast load q = 500 kPa, Biot option not used, drained soil behaviour

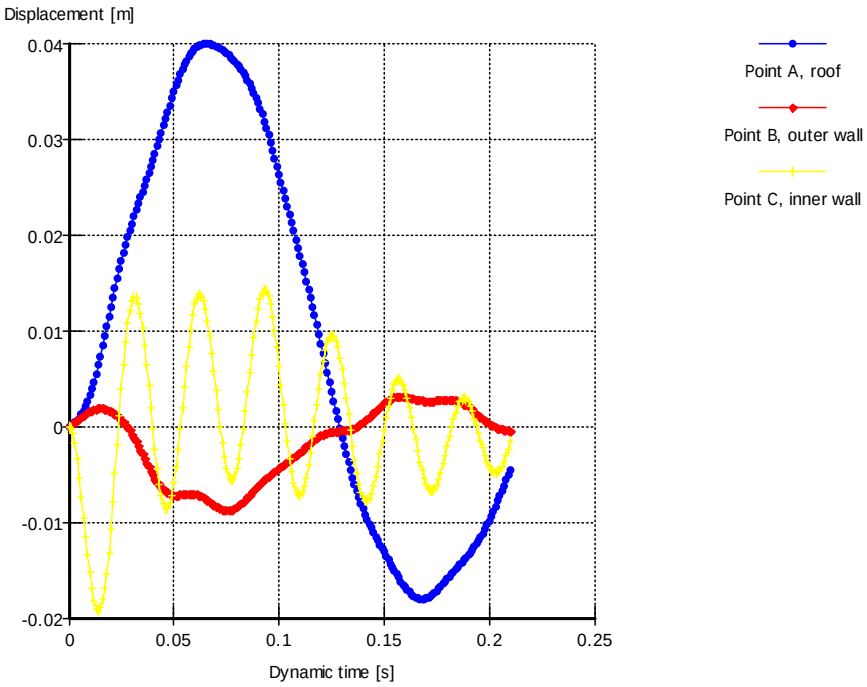

Figure 5.8 Tunnel response, blast load q = 500 kPa, Biot option not used, undrained soil behaviour

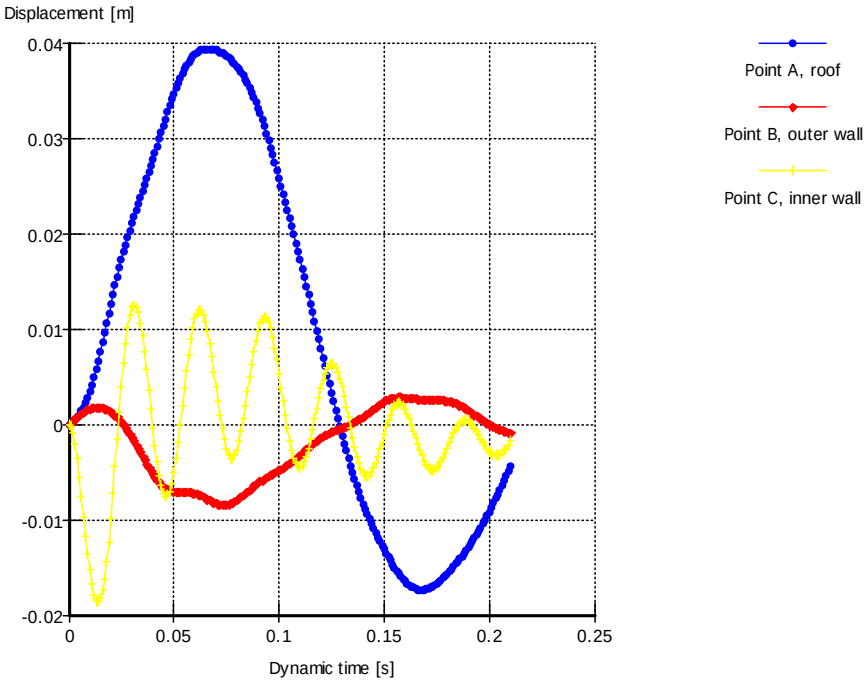

Figure 5.9 Tunnel response, run3, blast load q = 500 kPa, Biot option used

The outer wall at first moves outward. After a short time the wall moves inward, against the explosion pressure. The bending of the roof is responsible for this, at first sight peculiar, behaviour.

The response of the tunnel in the calculation with undrained soil behaviour and in the calculation with the BIOT option is nearly the same. In the calculation with drained soil behaviour the deflection of the roof and outer wall is less. The response of the tunnel is less as for the situation without soil (see section 5.2).
In the undrained calculation the soil at top of the roof shows excess pore pressures. These influence the strength and stiffness of the soil. Next to the tunnel underpressures develop.

The coordinates for which the soil response is given are given in table 5.2. Point H is below the tunnel. Points I, J and K are located on top of the tunnel (top of roof at y = -2m), at mids of the roof. Points L to Q are located next to the tunnel (wall at x = 16.8 m) at half height.

point	x	y	remark
H	8.99	-10.76	0.26 m below tunnel
I	8.15	-1.86	0.14 m above tunnel
J	8.15	-1.46	0.54 m above tunnel
K	8.37	-1.04	0.96 m above tunnel
L	16.9	-6.34	0.10 m next to tunnel
M	17.28	-6.63	0.48 m next to tunnel
N	17.61	-6.24	0.81 m next to tunnel
O	18.66	-6.40	1.86 m next to tunnel
P	19.73	-6.61	2.93 m next to tunnel
Q	21.89	-6.47	5.09 m next to tunnel

Table 5.2 Coordinates stress points for which response will be given

For calculation run3 the development of the shear strain is shown in figure 5.##. Shown is the equivalent shear strain. The definition of this strain is given in annex A.

A comparison of this shear strain definition with two other definitions is given in section 5.5 (run 5).

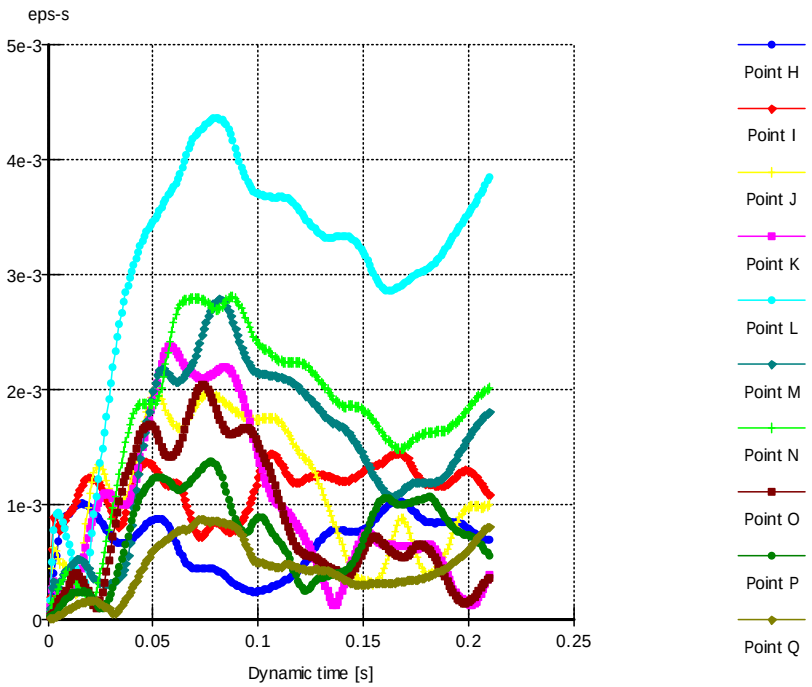

Figure 5.10 Development equivalent shear strain, run 3

The horizontal total soil stress outside the tunnel next to the wall is shown in figure 5.11. This time-stress curve may be compared with the applied loading inside the tunnel (see figure 2.2). The horizontal stress is at first a compression stress is present of nearly 450 kPa. The stress changes to a tension stress of 100 kPa.
The tunnel structure acts as a filter that decreases the load at the soil. In the extreme case of a perfect rigid and non-yielding tunnel the load at the soil is expected to be zero.

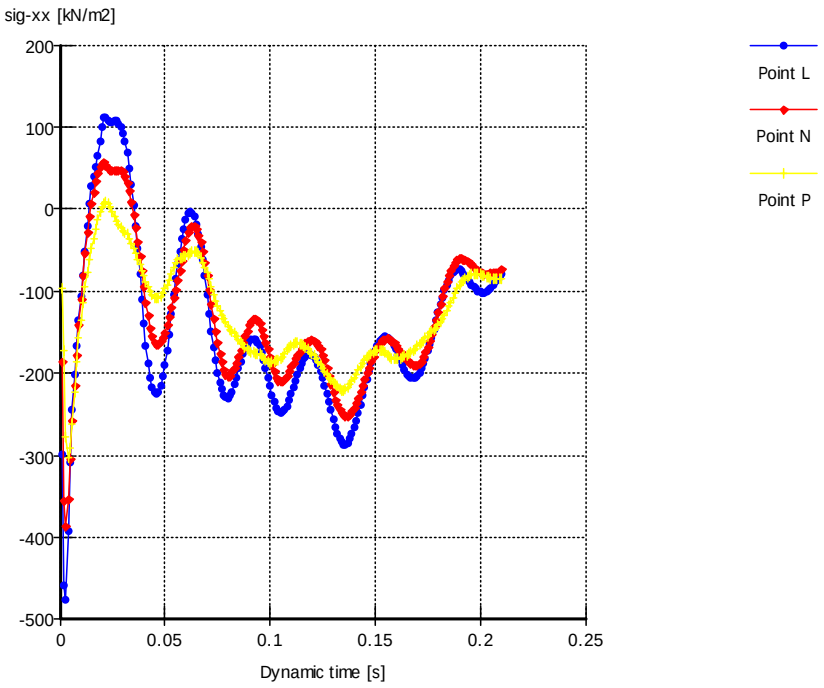

Figure 5.11 Development horizontal total stress next to the tunnel (positive stress is tension)

At point L the horizontal total stress at first drops from -63 kPa to -475 kPa and than increases to + 111 kPa.

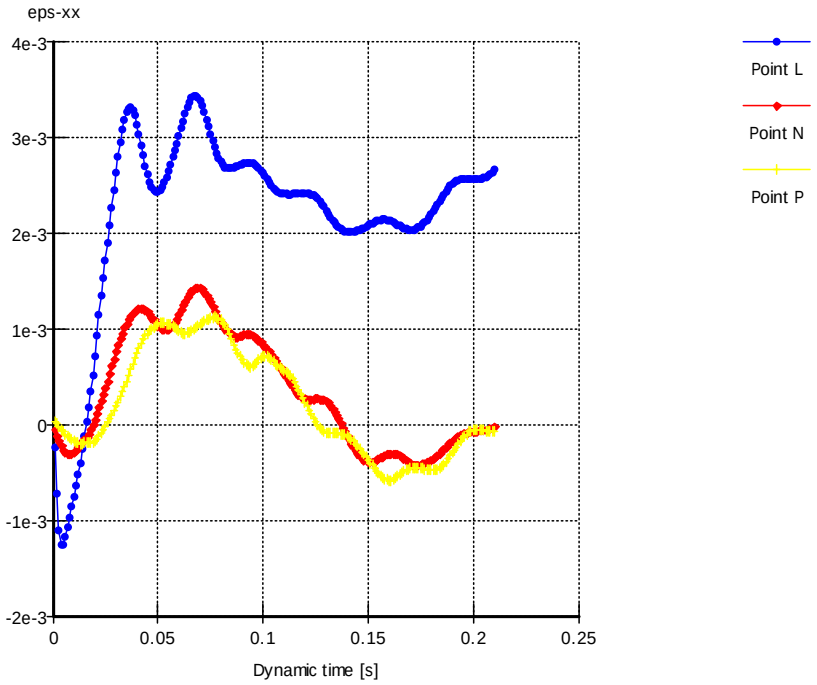

Figure 5.12 Development horizontal strain stress next to the tunnel, run 3

The strain rate of point L is about 0.4% in 0.03 s, so 13%/s.

5.4 Effect of magnitude blast load on tunnel and soil response

Calculation 4 serves to show the effect of a larger blast load on the tunnel and soil response.

The effect of the magnitude of the explosion load on the tunnel and soil response is investigated by performing a calculation with a higher load. The used load is given in figure 2.2.
Figure 5.13 shows the tunnel response and figure 5.14 the development of the shear strain in the soil.

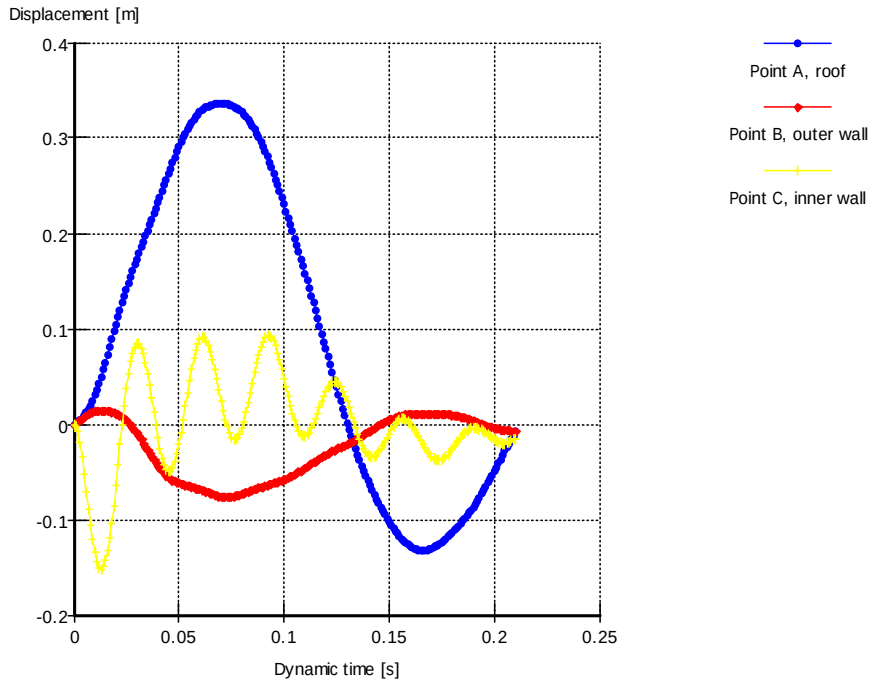

Figure 5.13 *Tunnel response, run 4, large blast load*

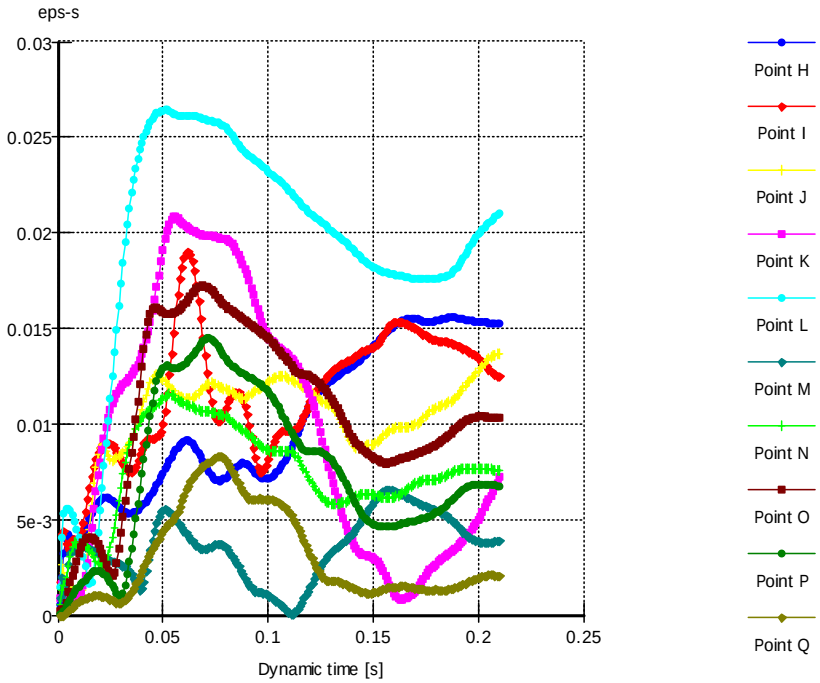

Figure 5.14 *Development equivalent shear strain around the tunnel, run 4, large blast load*

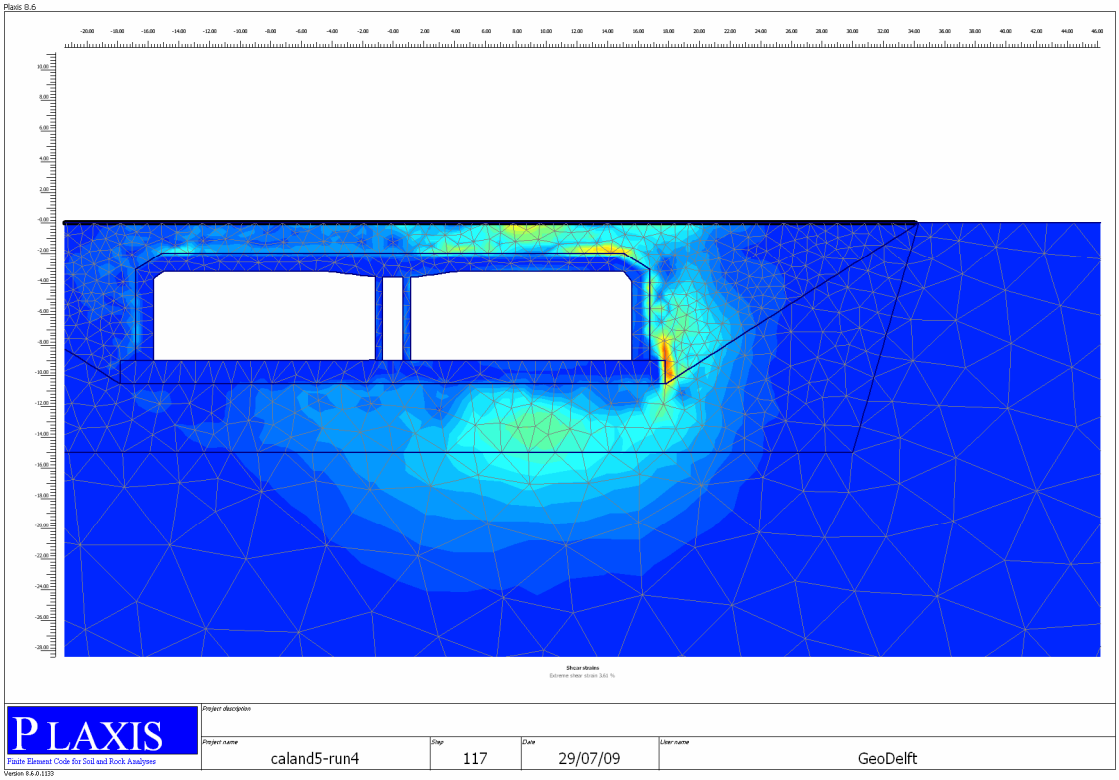

Figure 5.15 *Distribution equivalent shear strain around the tunnel, run 4, large blast load, t = 0.08 s, maximum value is 3.6%*

The response of the tunnel increases with a factor 15 to 20. The shear strains in the soil increase with a factor of 5 to 10.

5.5 Effect elasto-plastic concrete behaviour on tunnel response

Calculation 5 serves to show the effect of elasto-plastic tunnel behaviour on the tunnel response in PLAXIS. This calculation is to be compared with the TNO calculations with LS-DYNA

The previous calculations assumed a linear-elastic behaviour of the concrete. In this section it is investigated what the influence of using an an elasto-plastic material for the concrete is on the tunnel and soil response. The material parameters for the concrete are given I nsection 4.3.

Figure 5.16 shows the tunnel response.

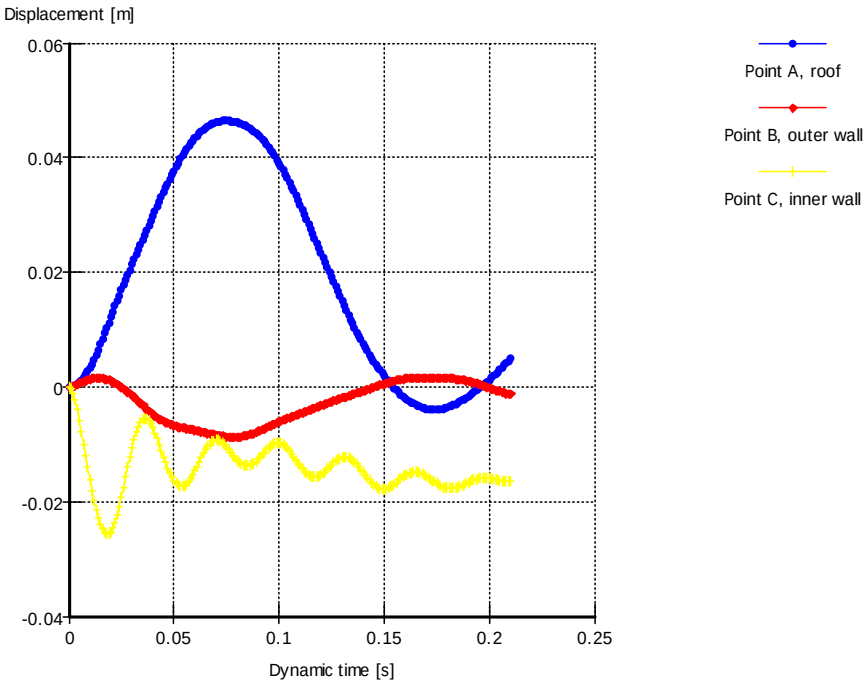

Figure 5.16 Tunnel response elasto-plastic tunnel

Figure 5.17 to 5.21 show the soil response at the selected points. The points are the same as used in section 5.3.

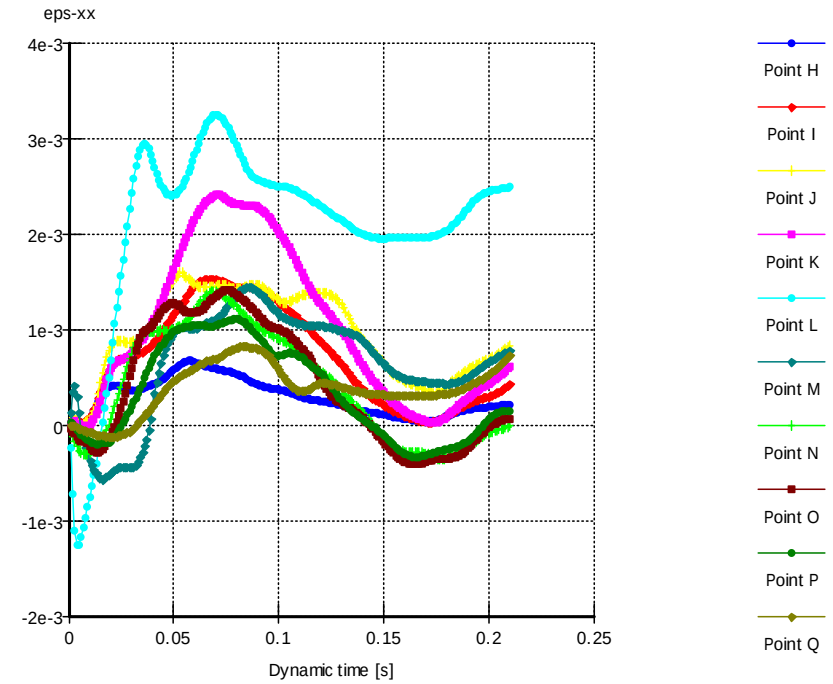

Figure 5.17 Development horizontal strain, run 5

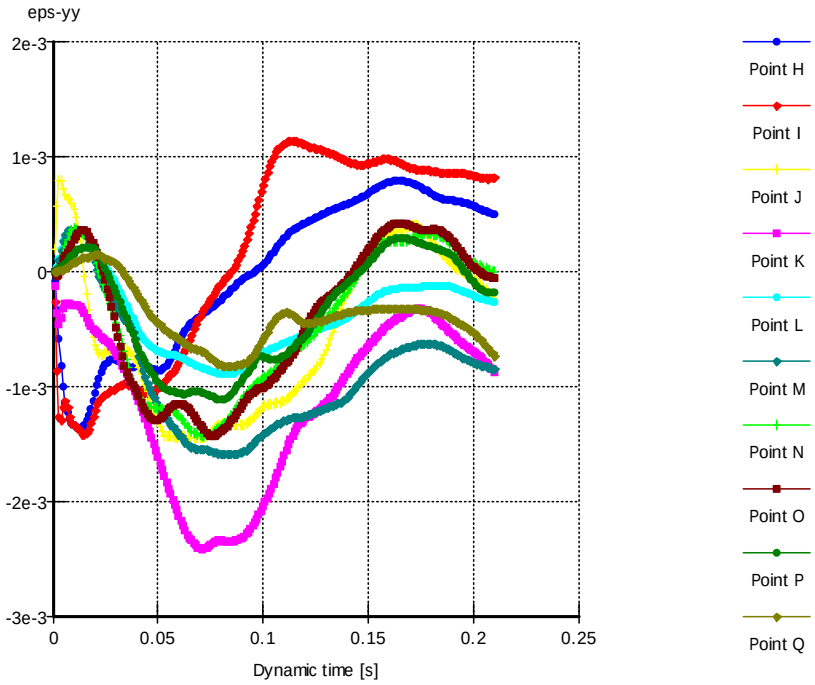

Figure 5.18 Development vertical strain, run 5

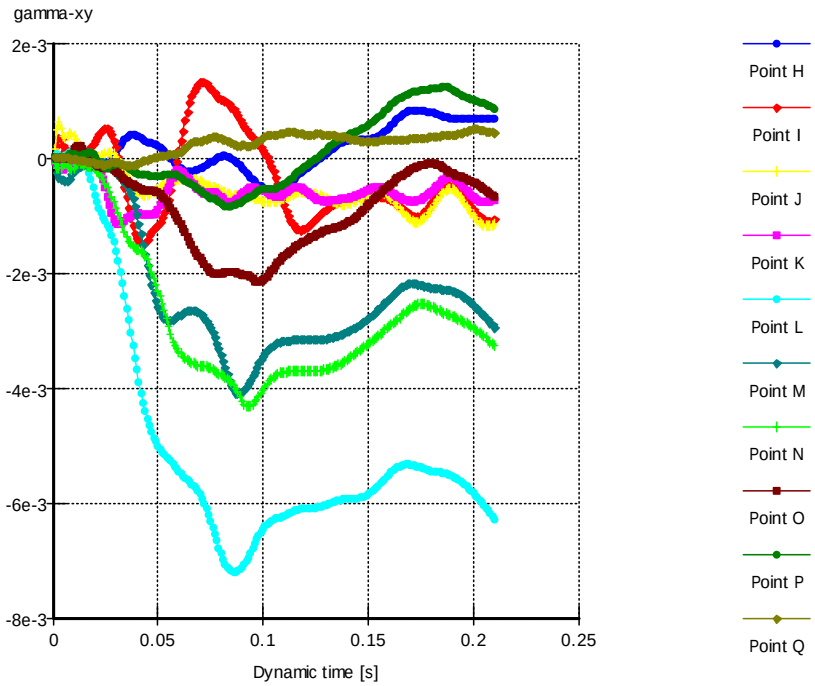

Figure 5.19 Development shear strain at xy-plane, run 5

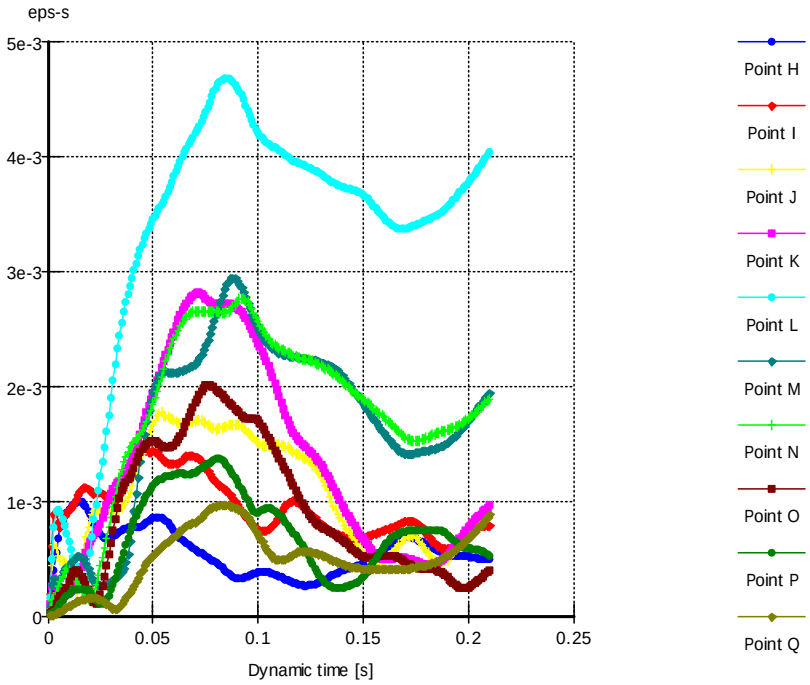

Figure 5.20 Development equivalent shear strain, run 5

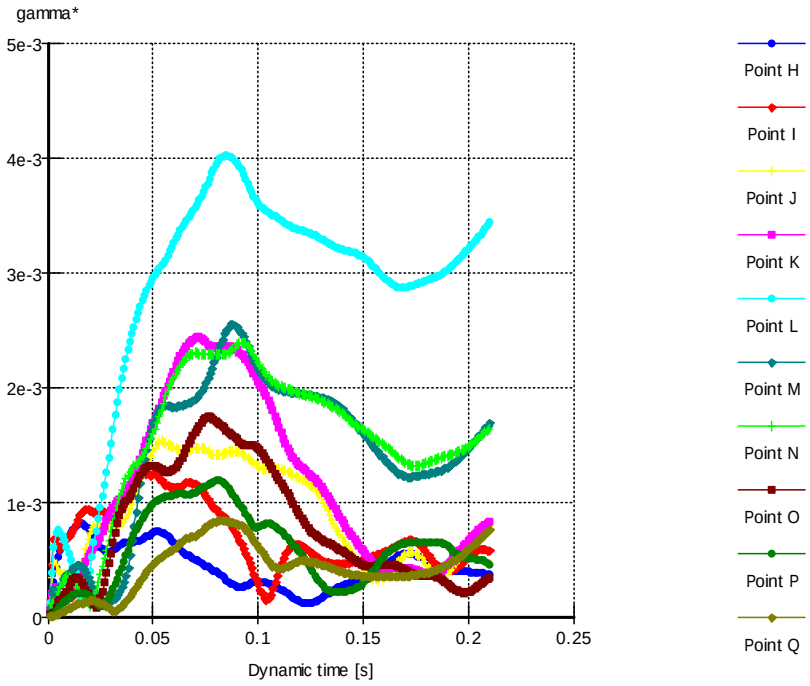

Figure 5.21 Development shear strain (radius Mohr's circle), run 5

The maximum shear strains occur at about t = 0.08 s. For this time step the distribution of the shear strains around the tunnel is shown.

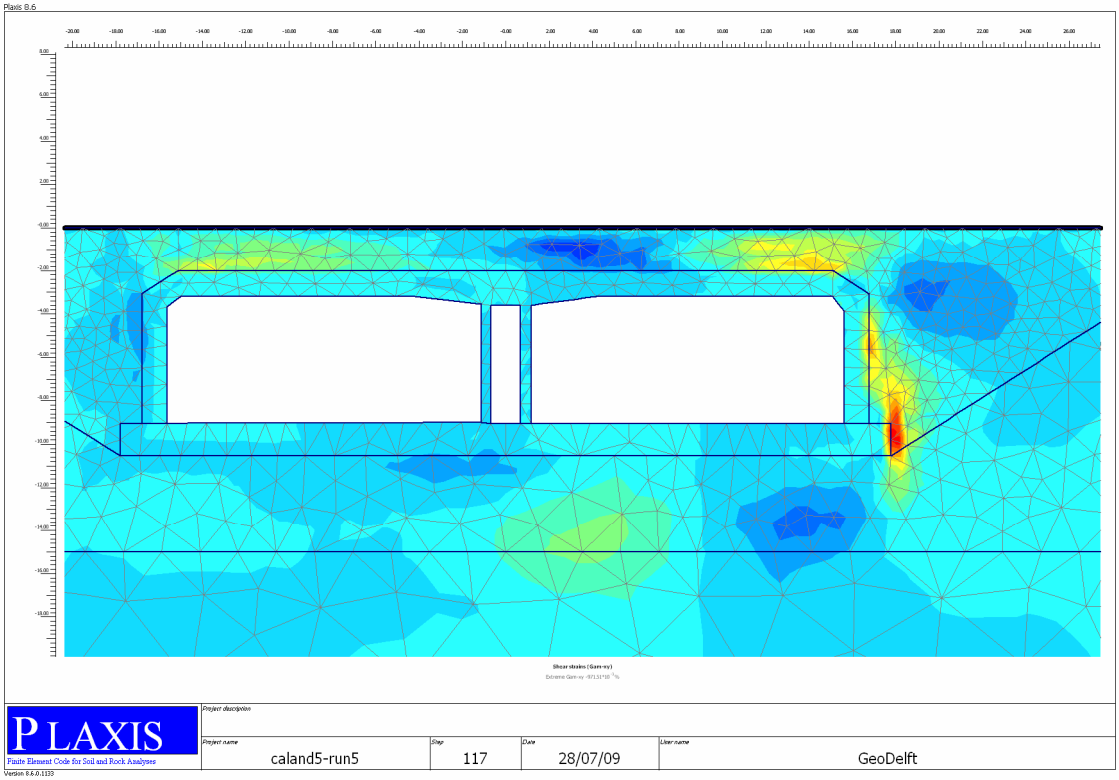

Figure 5.22 *Distribution shear strain gamma_xy at t = 0.08 s, value range is from varies between +0.4% to -1%*

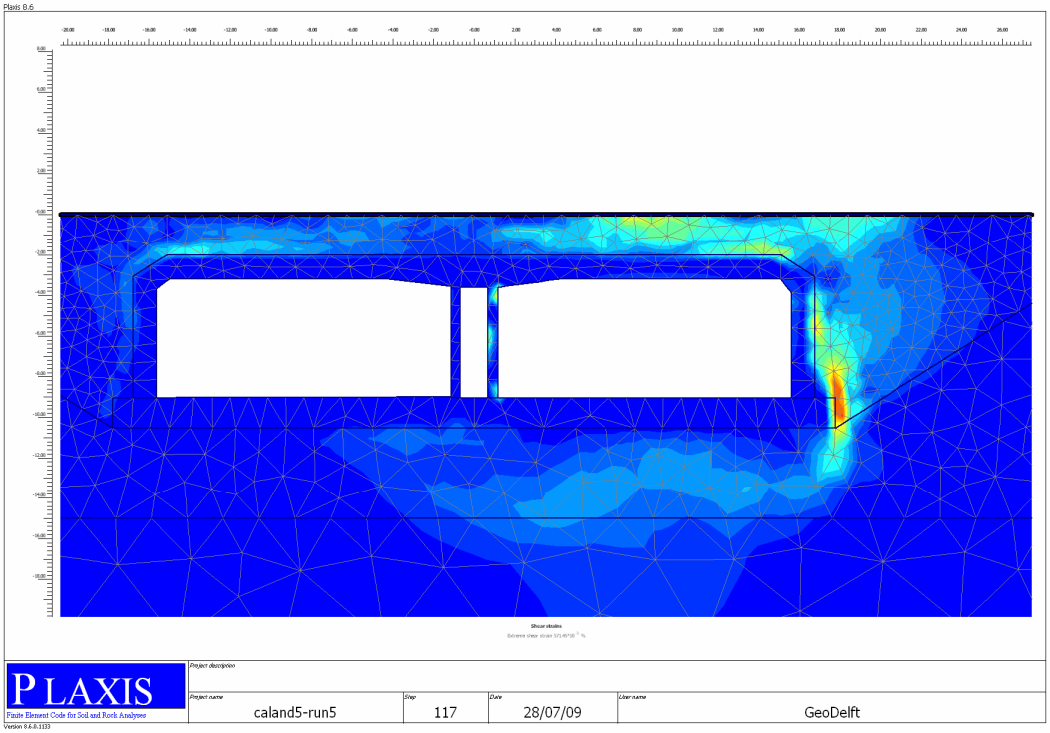

Figure 5.23 *Distribution equivalent shear strain at t = 0.08s, value range is from +0.6% to 0%*

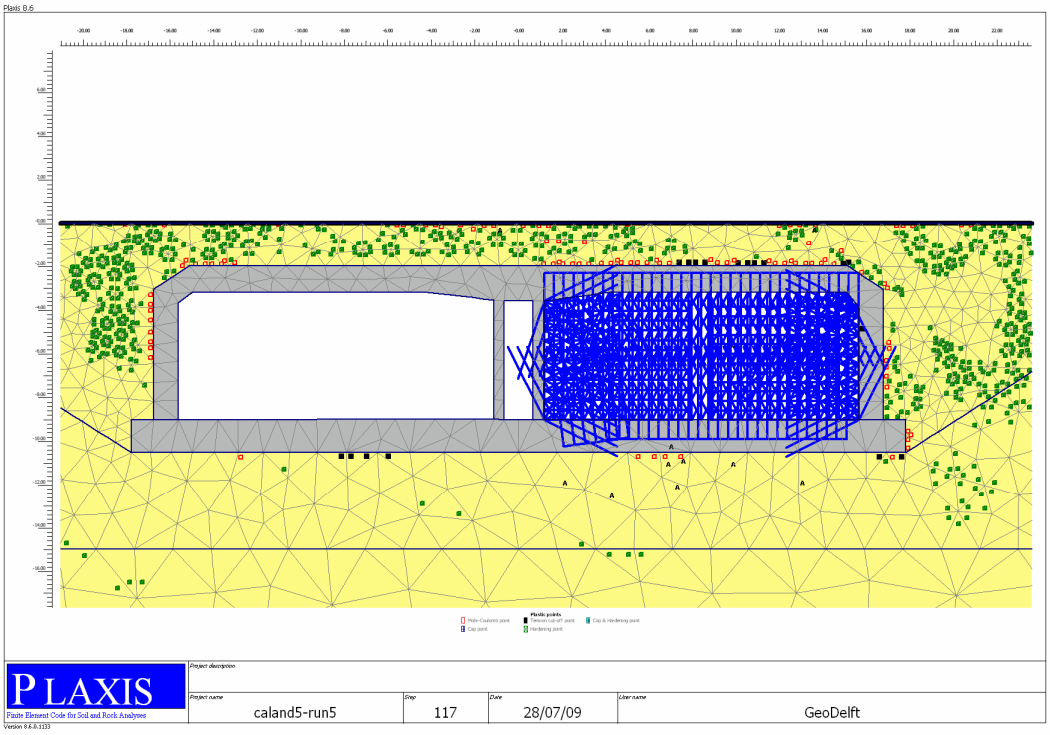

Figure 5.24 Plastic points at t = 0.08 s

In fact no plastic failure of the tunnel is observed in the PLAXIS calculation.

5.6 Effect of soil strength and stiffness on tunnel and soil response

Calculation 6 serves to show the effect of soil parameters on the tunnel and soil response.

In order to investigate the effect of the soil parameters on the soil and tunnel response a calculation with reduced strength and stiffness parameters is made. The following soil parameters are used:

- E_{50}^{ref} = 50 MPa
- E_{oed}^{ref} = 50 MPa
- E_{ur}^{ref} = 150 MPa
- ϕ= 30°
- ψ = 0°

For the tunnel an elasto-plastic material model is used. The results of this calculation are to be compared with the results presented in sections 5.5.
Figure 5.25 shows the response of the tunnel. Comparing this figure with figure 5.13 shows that there is no real difference in tunnel response.

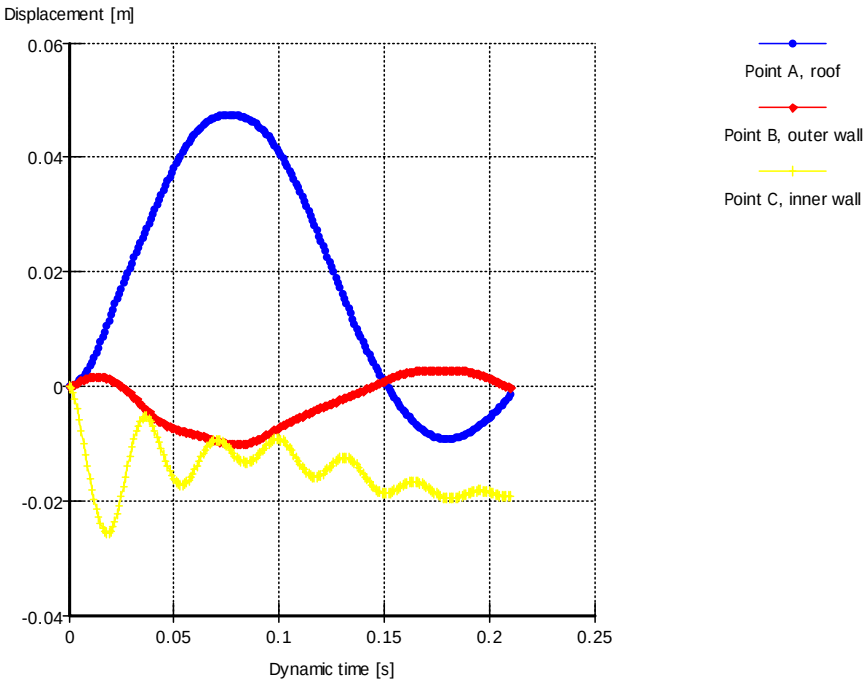

Figure 5.25 Tunnel response, run 6, reduced soil parameters, elasto-plastic tunnel response

Figure 5.26 shows the development of the shear strain in the 10 selected points and figure 5.27 the distribution of the shear strain at t = 0.08 s. The shear strains in the soil are increased, especially for the points M and N, located next tot the outer wall.

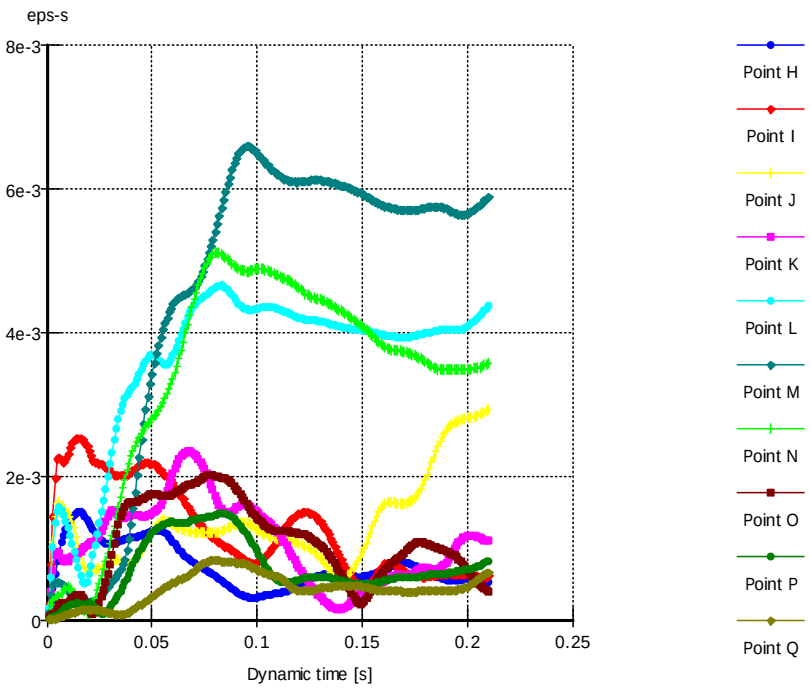

Figure 5.26 Development equivalent shear strain

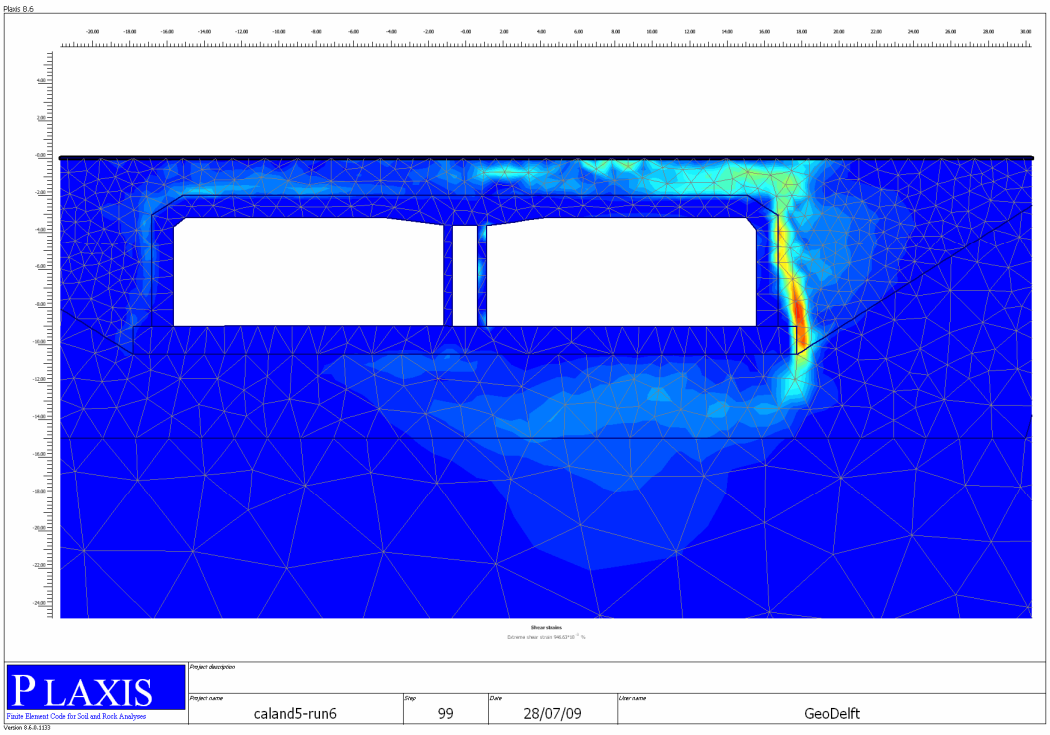

Figure 5.27 Equivalent shear strain at t = 0.08 s, maximum value is 0.95%

Figure 5.28 shows the plastic points at t = 0.08 s. With the reduced soil parameters only a small area with plastic concrete behaviour is present.

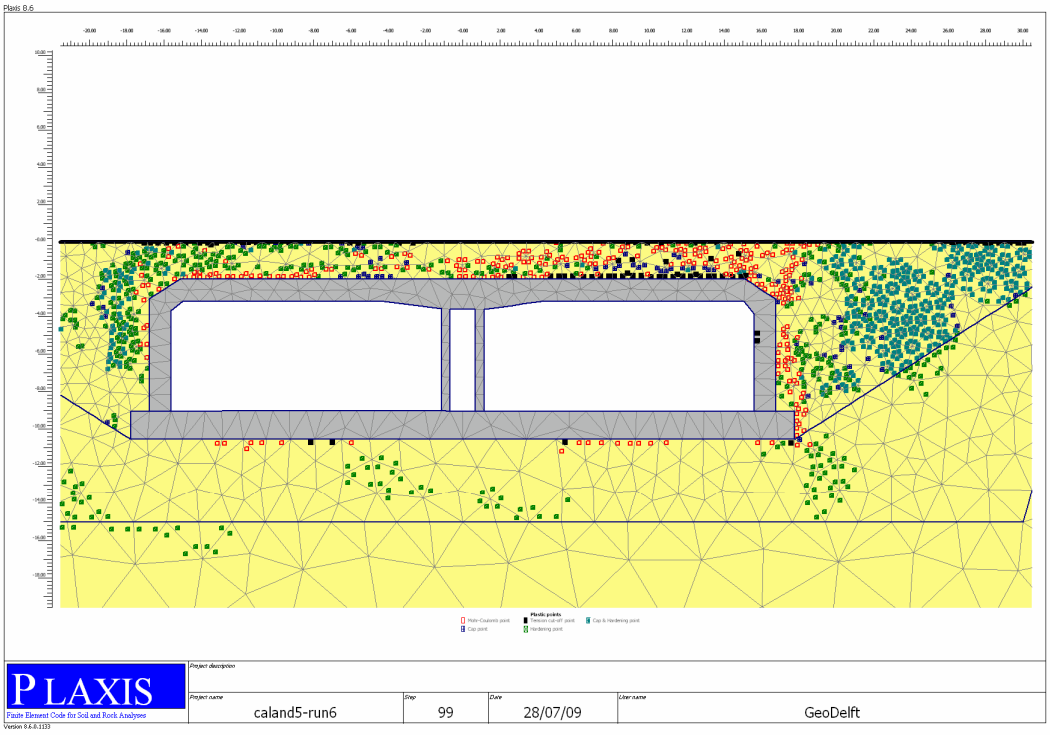

Figure 5.28 Plastic points at t = 0.08 s

6 Discussion on tunnel response

For the situation where the tunnel response remains essentially linear-elastic the tunnel can be well modelled in PLAXIS using volume elements.

When elasto-plastic behaviour of the tunnel (cracking of concrete) occurs the modelling of the tunnel in PLAXIS shows shortcomings, as cracking of the concrete cannot be properly modelled.

In the PLAXIS calculations, when using the recommended material parameters for concrete, the tunnel doesn't show any sign of plastic failure. This is in contradiction with the calculation results of TNO.

7 Discussion on soil response

7.1 Expected soil response from shear strain and triaxiaal test results

As part of the project a series of triaxiaal tests has been performed. From the results of the tests it is observed that at a vertical strain of 1 to 2 promille the soil behaviour becomes plastic.
Such a vertical strain in a triaxial test represents a shear strain. In PLAXIS different definitions for the shear strain are used and can be presented.
The shear strains in an undrained triaxial test may be expressed in these terms.
In an undrained triaxiaal test the volume strain is zero. This implies that the radial strain can be expressed as a function of the vertical strain:

$\varepsilon_{rad} = -0.5\varepsilon_{vert}$

The shear strain γ_{xy} is zero,
Using these relations the maximum shear strain, the deviator strain and gamma* can be expressed as a function of the vertical strain. This yields:

$\gamma_{max}=1.5\varepsilon_{vert}$
$\varepsilon_s \approx 0.8\varepsilon_{vert}$
gamma* = $0.75\varepsilon_{vert}$

Using these definitions it may be stated that plastic soil behaviour is present for a deviatoric strain in excess of about 1 promille. The calculation results show that an area of several meters around the tunnel shows shear strains in excess of this value.

The performed triaxial tests also show that in loose sand excess pore pressures remain after loading and unloading.

From the above it is concluded that excess pore pressures around the tunnel may be present after the blast.

7.2 General

The presently available soil models in PLAXIS do not correctly describe the loading-unloading behaviour. The model predicts a decrease in pore pressure during unloading. This is consistent with the assumed linear-elastic behaviour during unloading, combined with the assumption that the total effective stress doesnot change in undrained soil loading.
This loading-unloading behaviour may be considered as the first half cycle in a cyclic test. From undrained cyclic triaxial tests it is known that pore pressures develop during loading.

The consequence is that the excess pore pressures at unloading and afterwards are underpredicted. For the time of the blast the soil reaction is expected to be correctly modelled. For the time after the blast the pore pressures are larger as calculated. When the pore pressures below the tunnel increase there will be a risk of floatation of the tunnel. If this will occur depends on the amount of dilation during the blast and as such on the density of

the sand. For submerged tunnels the layer just below the tunnel is loose and therefore this risk cannot be excluded at the moment.

Other mechanisms that are not covered by the presently available constitutive models are:

- static liquefaction
- cyclic liquefaction

Static liquefaction is the mechanism that due to a sudden (small) change in shear stress or shear strain the soil skeleton collapses and the soil behaves as a fluid. Cyclic liquefaction is caused by cyclic loading. In loose sand and a sufficient high shear stress amplitude this may occur in one or two cycles. The development of the shear strain (see e.g. figure ??) shows that one or two cycles are present during an explosion.

7.3 Summary, conclusions and consequences

The present available constitutive soil models underestimate the risk of large excess pore pressures.

The calculated shear strains around the tunnel indicate that a zone of several meters around the tunnel may show excess pore pressures after the blast. It is not necessary that complete liquefaction will occur. Limited excess pore pressures already may endanger the stability of the tunnel.

The possible consequences of liquefaction for the tunnel can only be hypothesed. It is most likely that the tunnel starts to move upwards. In order to keep the upward pressure intact water and liquefied soil is to flow to the area below the tunnel. During this process, which will take time, excess pore pressures start to dissipate. Full floatation of the tunnel is therefore not expected, but displacements may become too large. The amount of vertical displacement can therefore only be guessed. Horizontal displacements are expected to be limited.

Dissipation of excess pore pressures from the zone next to the tunnel may increase the pore pressure in the surrounding after the blast. This may have consequences for the stability of surrounding structures as buildings, pipelines, etc.

Conclusions

Simulations of the performed triaxial test results show that the available constitutive soil model in PLAXIS describes the loading branch reasonable. However the unloading behaviour in the PLAXIS simulations is completely different from the observed behaviour at unloading. Further study on the constitutive modelling must focus on the unloading branch.

The tunnel response in the PLAXIS calculations when using volume elements is in fair agreement with the response as derived by TNO for a calculation with DIANA and using beam elements. A requirement is that sufficient volume elements are used.

The difference in tunnel response for a calculation with and without Biot is limited, a large difference is observed between the calculation with drained and with undrained soil behaviour. The advantage of using the Biot option seems limited for this stage.
For the behaviour (displacements) of the tunnel after the explosion the Biot option is usefull. The presently available constitutive models do not cover into account some relevant mechanisms. The calculated amount of excess pore pressure is therefore expected to be underpredicted.

Indications are that the soil strength and stiffness only have a marginal influence on the tunnel response during the blast. For the behaviour after the blast the parameters may be of significance. The shortcomings of the presently available constitutive models however already make the calculated soil response questionable.

When a clear insight in the soil stresses close to the tunnel is required small elements close to the tunnel are required. The advantage of using the PTU/PMU option therefore appears to be limited for the soil-tunnel interaction response calculations.

References

[Al-Khoury Weerheijm 2009]
Delft Cluster Project C31D03, Sub-work Package R2, Numerical Modeling of Soil Behavior under Blast Loading
TU Delft, June 2009

[Hölscher 2006]
Hölscher, P.,
Kennisleemtes in de Geotechniek bij dynamische belastingen in tunnels, voorstudie
Deltares report 418420-0013, version 2, June 2006

[Meijers 2007]
Static and dynamic undrained triaxial tests on sand
GeoDelft report 418420.0026, September 2007

[Meijers 2009]
DC COB Bijzondere belastingen, Validation implementation Biot in PLAXIS
Deltares report 1001136-007-GEO-0001, October 2009
[PLAXIS]
PLAXIS version 8, material models manual

[Vervuurt et al 2007]
Vervuurt, A.H.J.M., Galanti, F.M.B., Wubs,A.J., Berg,A.C. van den,
Effect of explosions in tunnels, Preliminary assessment of the structural response
TNO report 2007-D-R0156/A, April 11, 2006

ANNEX A DEFINITION SHEAR STRAIN COMPONENTS IN PLAXIS

The definitions of the strain components are:

$$\varepsilon_s = \sqrt{\tfrac{-4}{3} J_2}$$

$$J_2 = \varepsilon_{xx}\varepsilon_{yy} + \varepsilon_{yy}\varepsilon_{zz} + \varepsilon_{xx}\varepsilon_{zz} - \tfrac{1}{4}\gamma_{xy}^2 - \tfrac{1}{4}\gamma_{yz}^2 - \tfrac{1}{4}\gamma_{xz}^2$$

For a plane strain situation the strains ε_{zz}, γ_{xz} and γ_{zy} are zero. The second invariant becomes:

$$J_2 = \varepsilon_{xx}\varepsilon_{yy} - \tfrac{1}{4}\gamma_{xy}^2$$

The parameter gamma* is the radius of the Moh's circle in the x-y plane. This gives:

$$gamma^* = \sqrt{\tfrac{1}{4}(\varepsilon_{xx} - \varepsilon_{yy})^2 + \tfrac{1}{4}\gamma_{xy}^2}$$